Multiscale transforms: application to CMB, secondary anisotropies and infrared spectra of Mars surface

Olivier Forni
Institut d'Astrophysique Spatiale
Université Paris-Sud, Orsay
France

The Cosmic Microwave Background

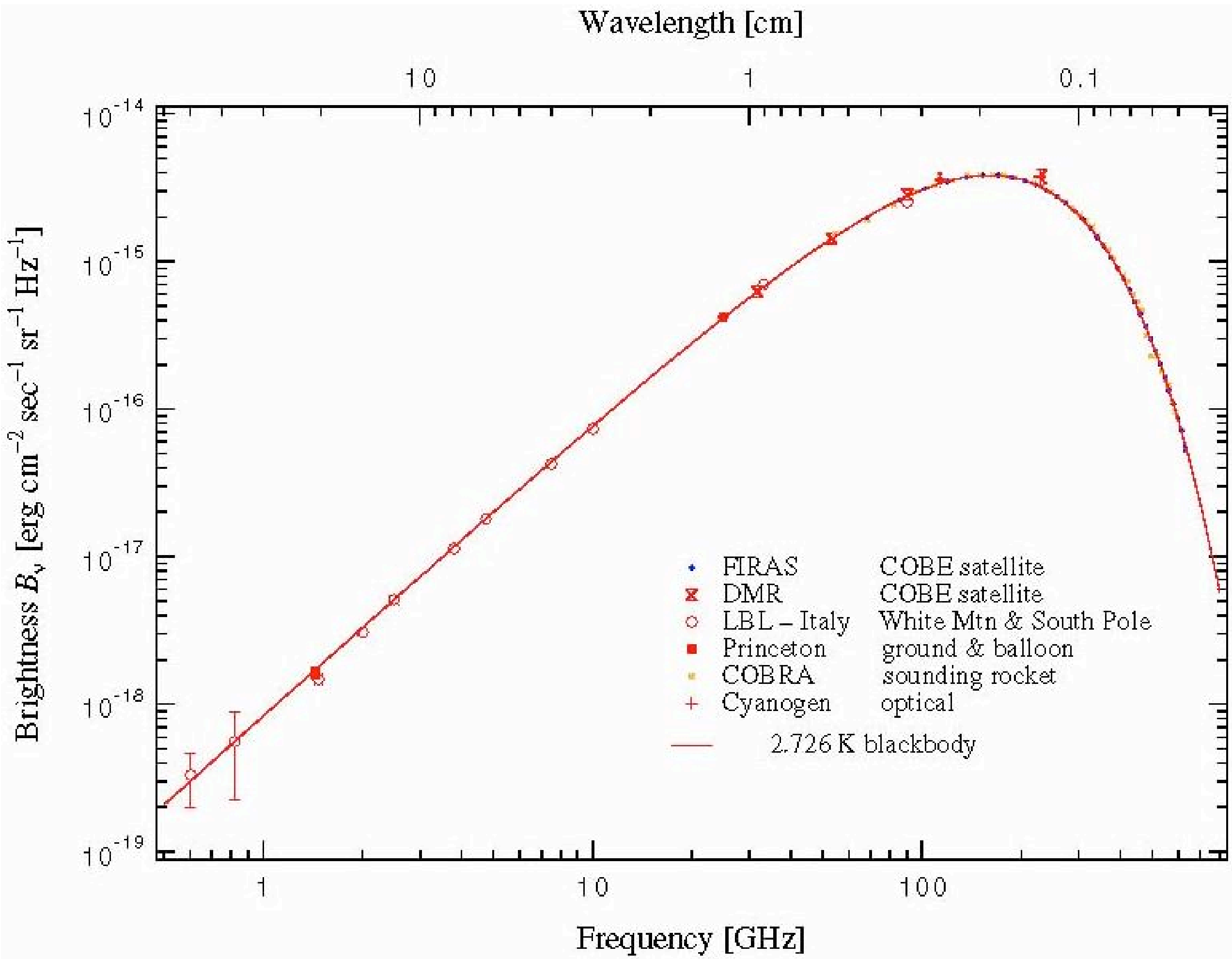

The Cosmic Microwave Background

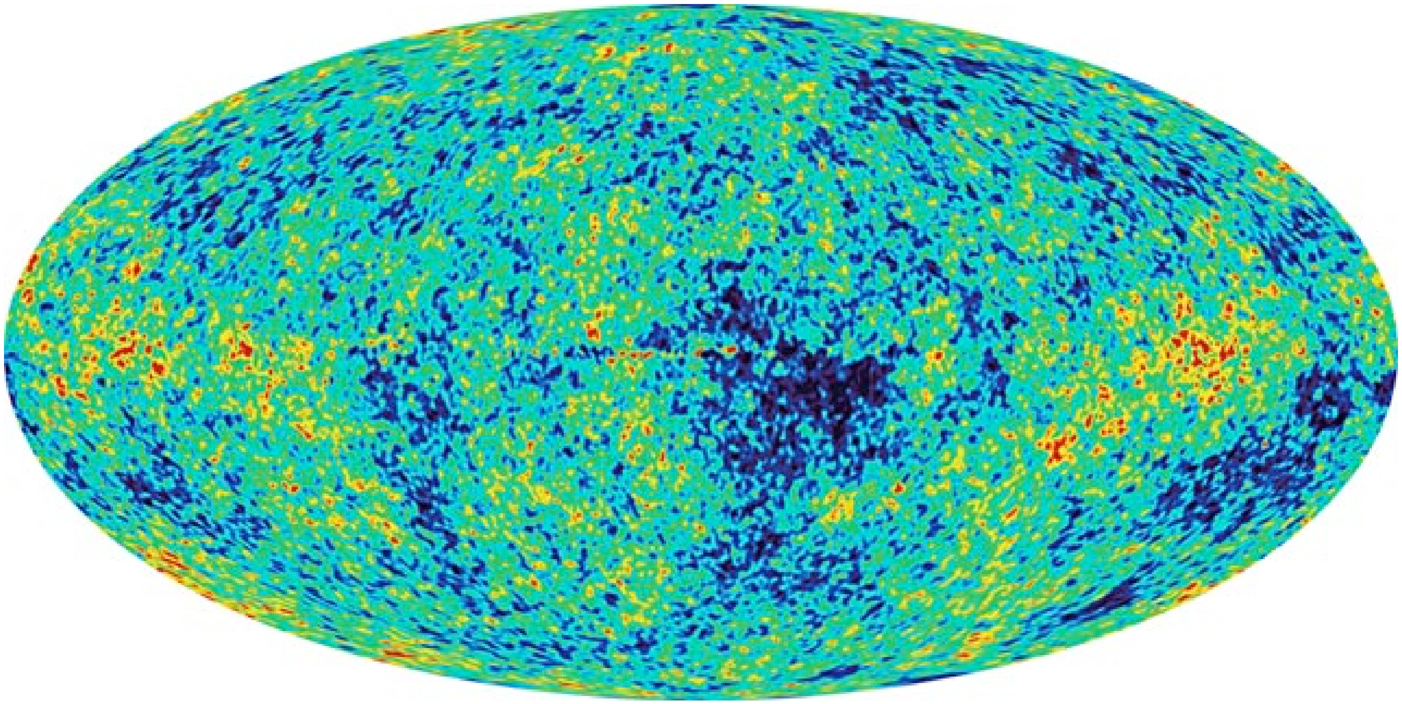

Where do these primary fluctuations come from ?

The Cosmic Microwave Background

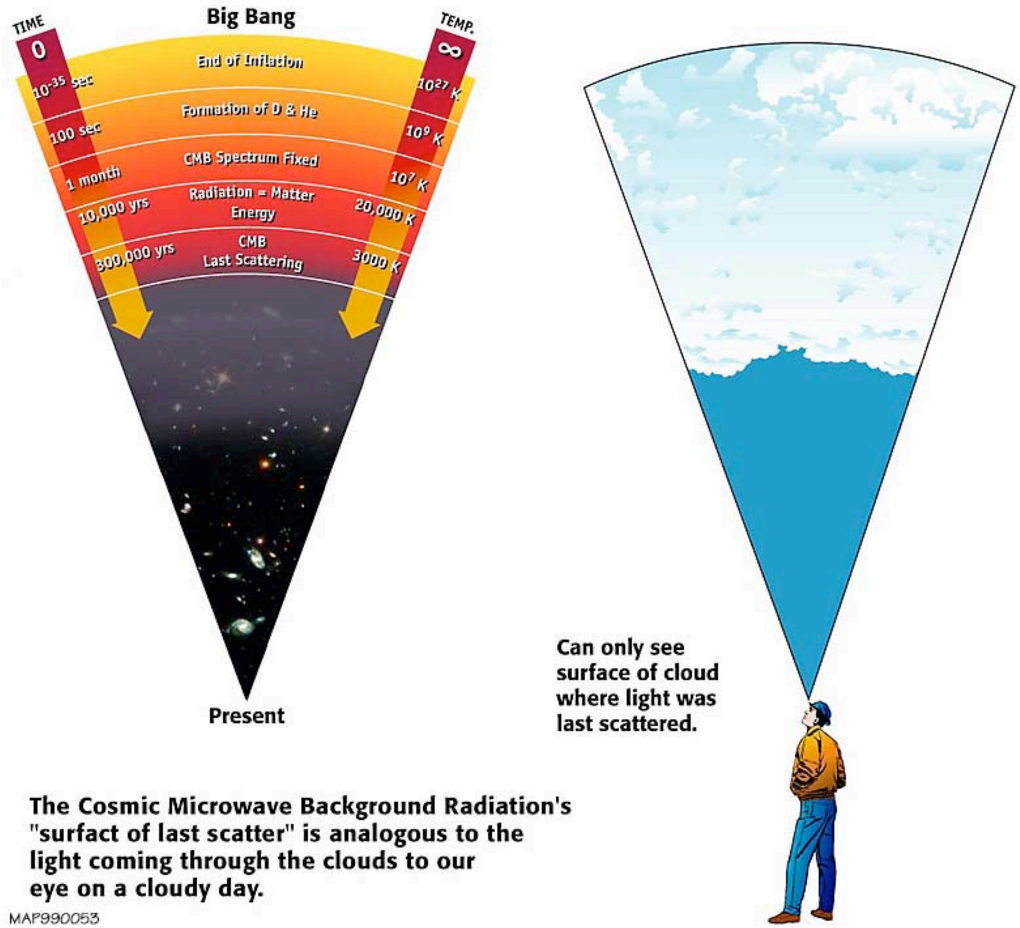

The Cosmic Microwave Background

- The power spectrum gives constrains on the geometry and physical state of the Universe.
- It supports the hypothesis of a period of rapid expansion of the early Universe: the Inflation period.

The Primary fluctuations

• Inflation causes random distributed density seeds and Gaussian distributed fluctuations.

• Non-linear coupling between fluctuations can generate non-Gaussian signatures.

•At the end of this period, topological defects can occur that produce non-Gaussian fluctuations e.g. Cosmic Strings.

The Secondary fluctuations

The secondary fluctuations arise from the interaction of the CMB photons with the interleaved matter or structures.

- The Sunyaev Zel'dovich (SZ) effect.
- Gravitational lensing by large scale structures.

The Sunyaev Zel'dovich effect

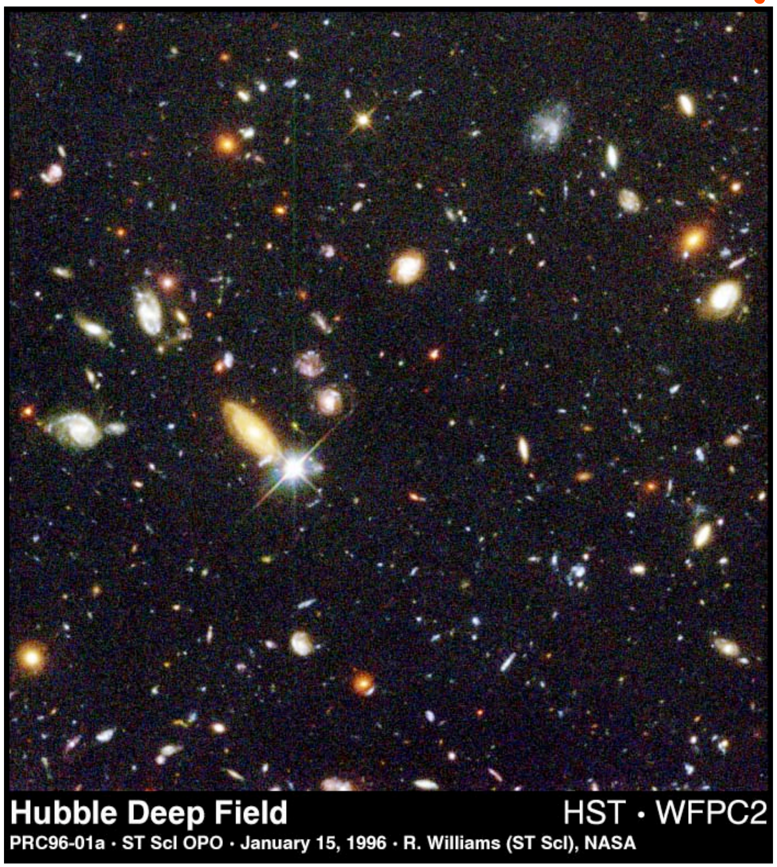

The SZ effect comes from the interaction of the cold CMB photons with the hot electrons (TSZ) of moving (KSZ) galaxy clusters

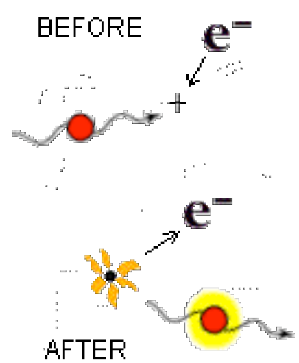

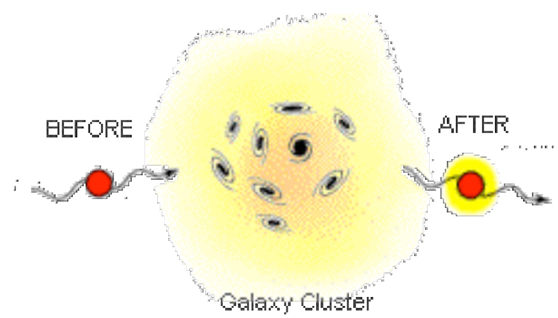

The Sunyaev Zel'dovich effect

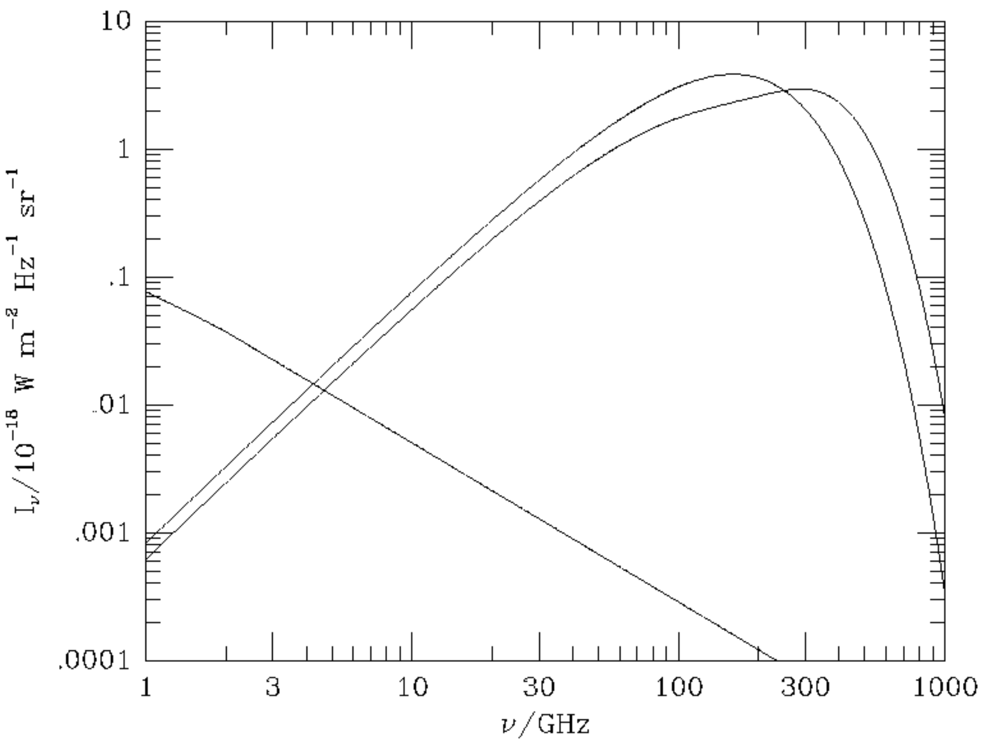

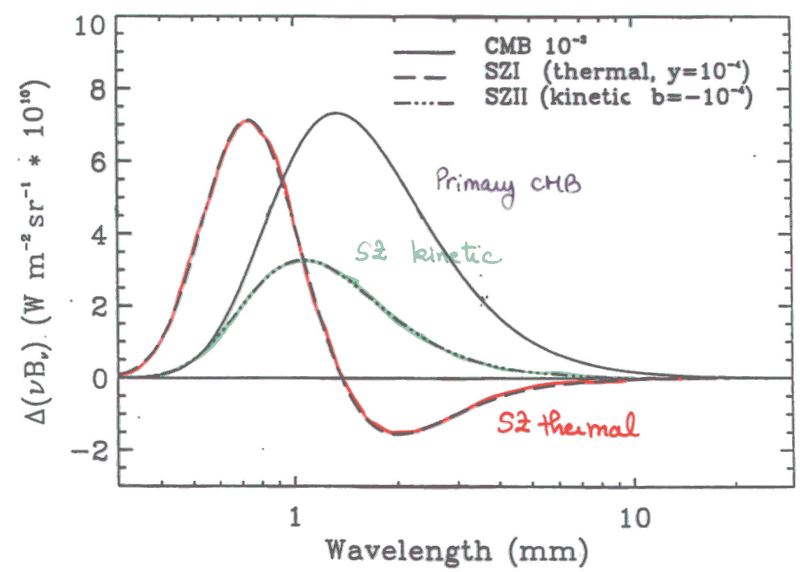

Frequency dependence of Thermal SZ
=> Allows component separation

The Sunyaev Zel'dovich effect

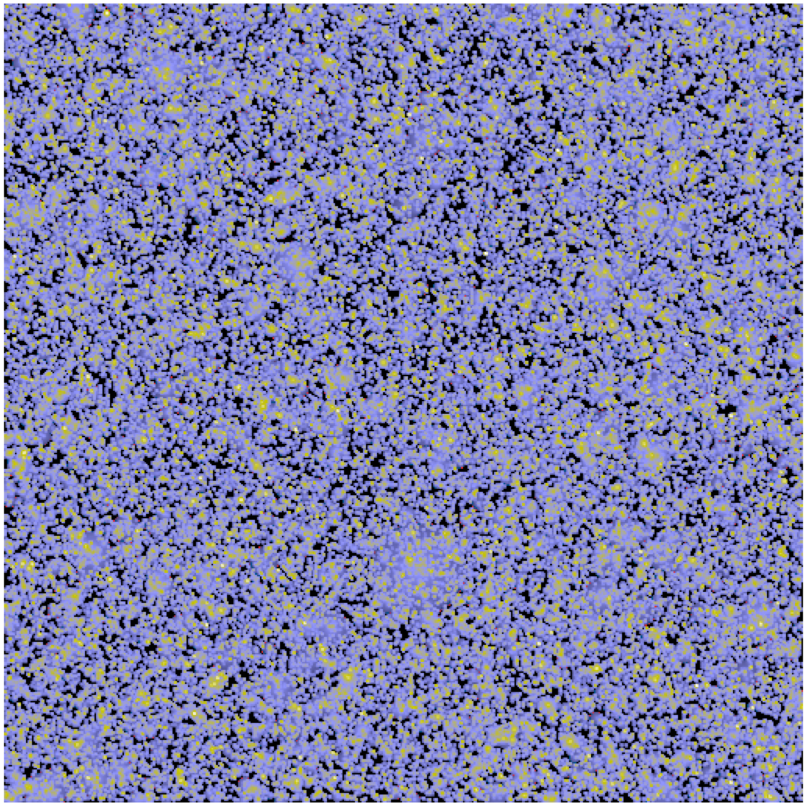

Thermal SZ

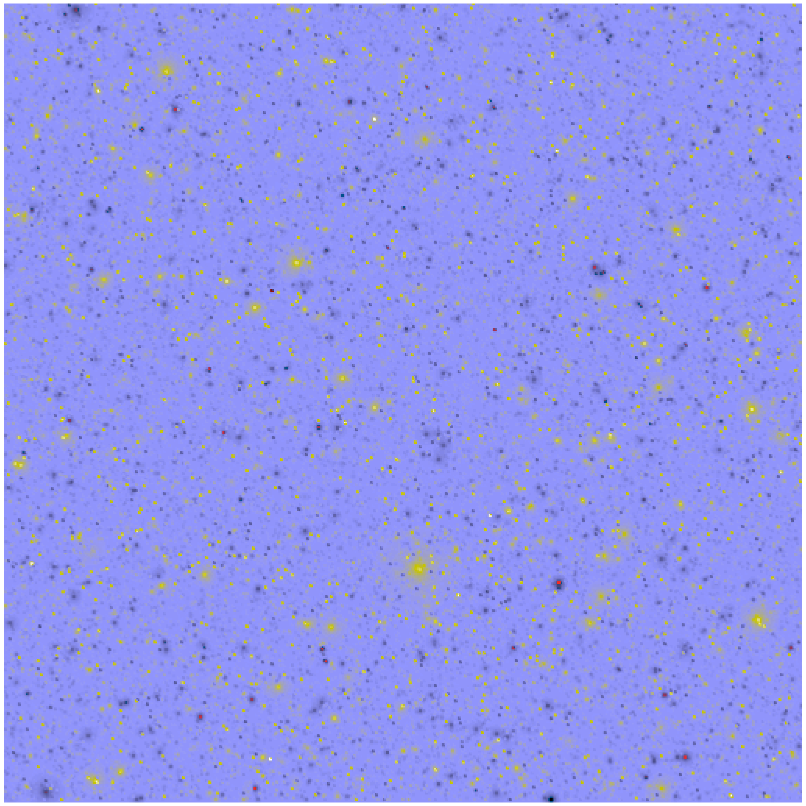

Kinetic SZ

Lensing

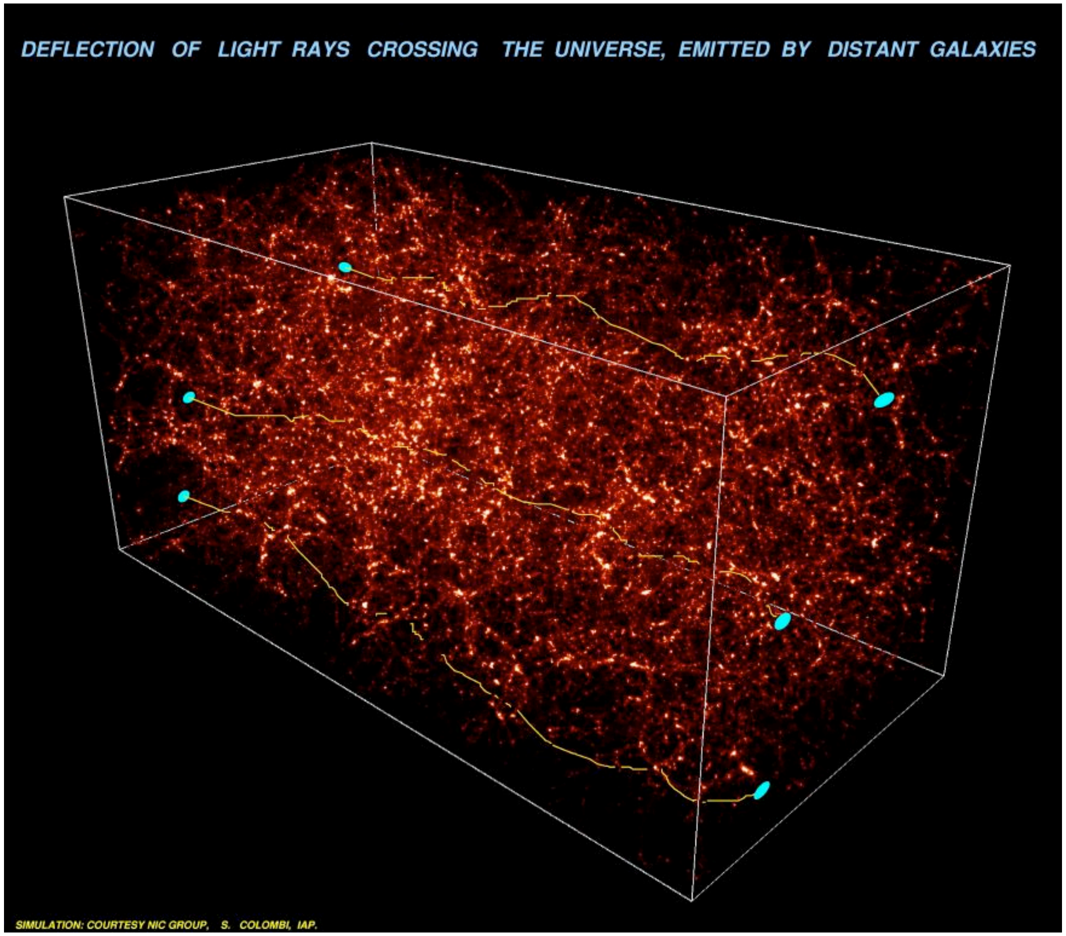

CMB photons are deflected by the mass of large scale structure => the CMB exhibit a deformation

Lensing

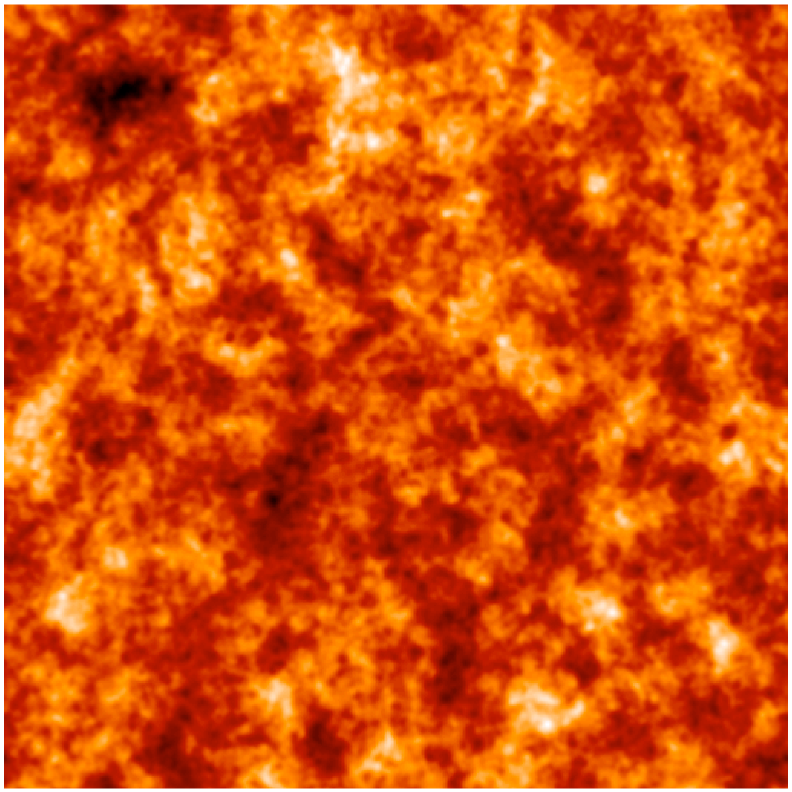

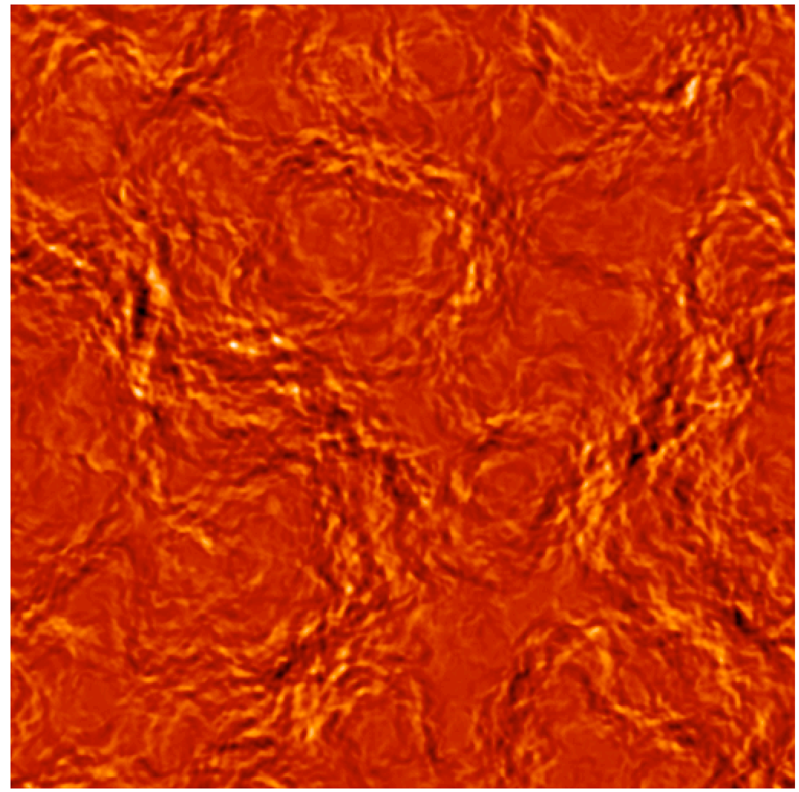

The other contributions

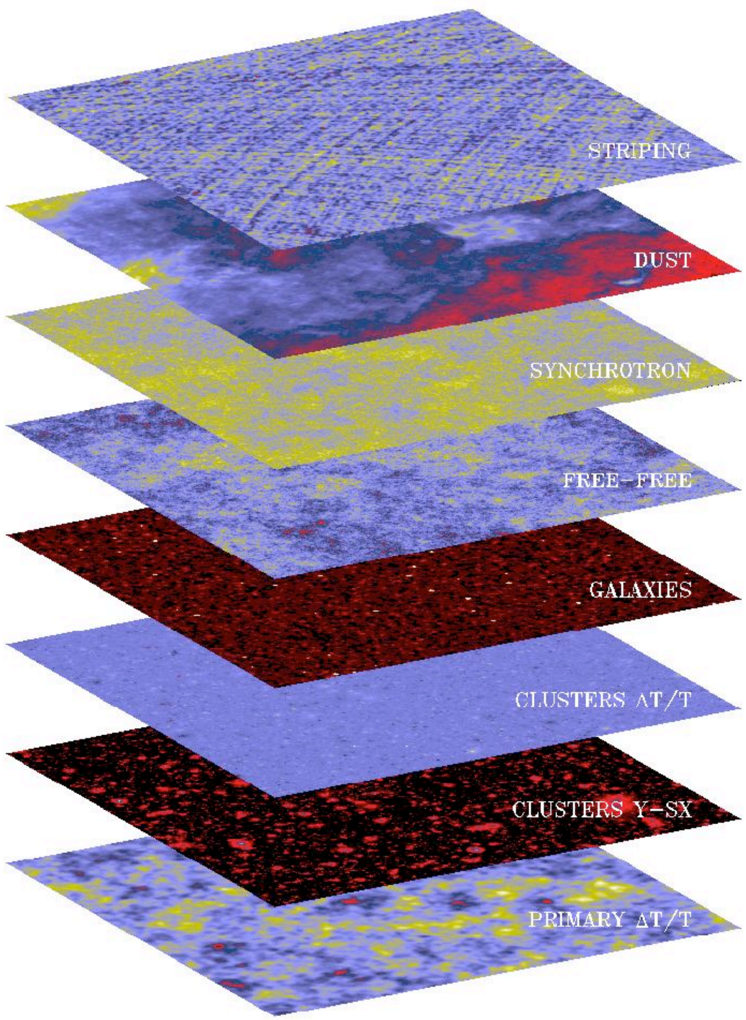

F.R. BOUCHET & R. GISPERT 1998

Besides the secondary fluctuations, other foreground fluctuations contribute to the signal, the Galaxy, the dust emission from interstellar clouds. Finally observation strategy and/or instrumental systematics corrupt the final signal.

Questions

1. Can we detect a non-Gaussian signal embedded in a dominant Gaussian one ? (Aghanim & Forni, Forni & Aghanim, 1999)
2. How do multiscale analysis compare with N point correlation functions ? (Aghanim, Kunz, Castro & Forni, 2003)
3. Can we discriminate between two (or more) non-Gaussian signals? (Starck, Aghanim & Forni, 2004)
4. Can we separate the non-Gaussian signal from the dominant Gaussian one (Forni & Aghanim, 2004)

Can we detect ?

Simulated signals taken in this study

- Primary fluctuations
  - Gaussian field resulting from inflation

- Secondary fluctuations
  - Sunyaev Zel'dovich effect

512x512 pixels maps : 1.5'/pixel

CMB

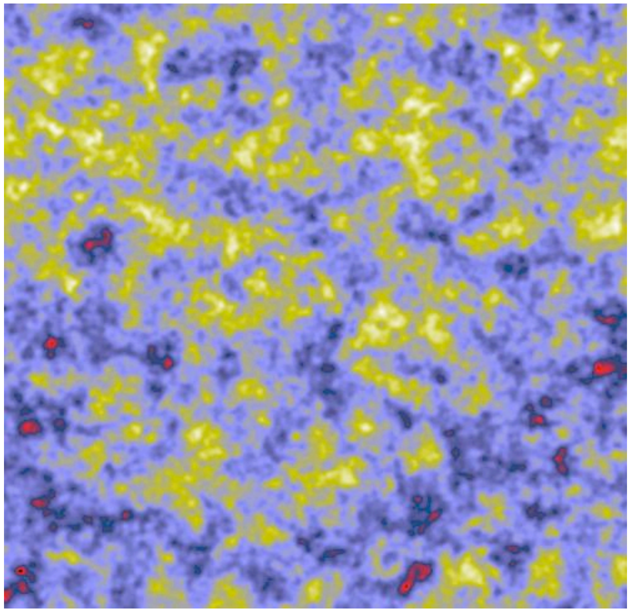

SZ

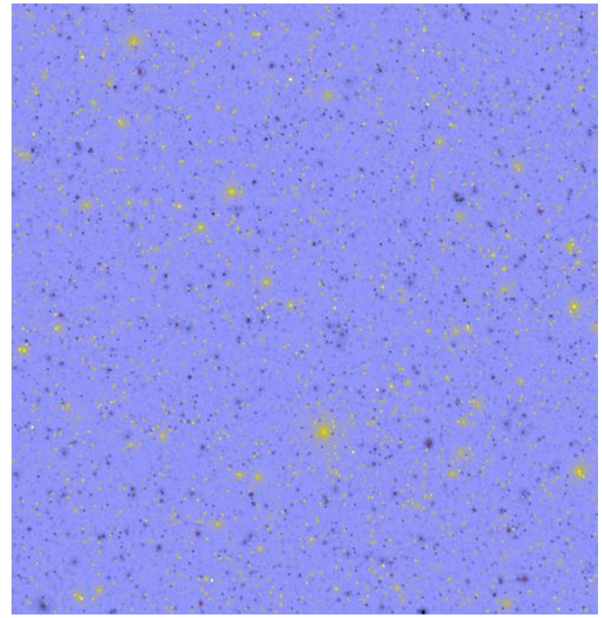

Total

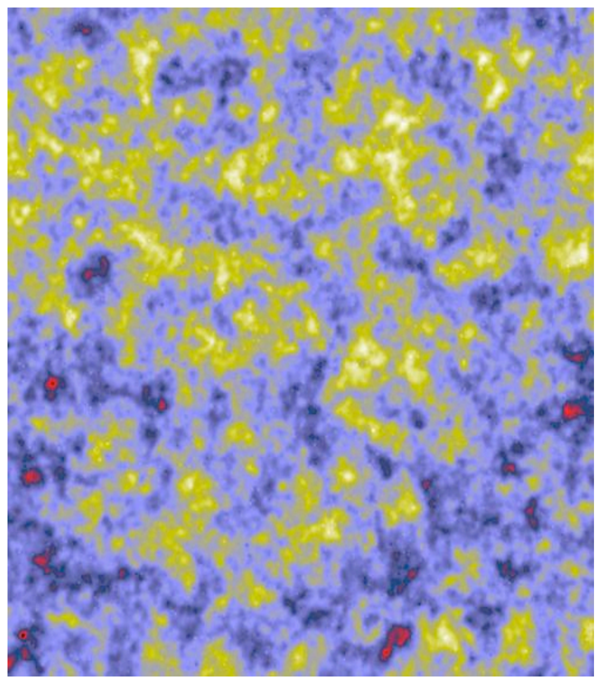

Methodology

Two types of data set are analysed

1. The non-Gaussian data set
2. A Gaussian data set having the same power spectrum as the non-Gaussian one.

- Bi-orthogonal transform is performed on both data sets
- The resulting moment of the coefficient distribution are compared using a Kolmogorov-Smirnov test.
- This test gives a probability of detection.

Bi-orthogonal wavelet transform

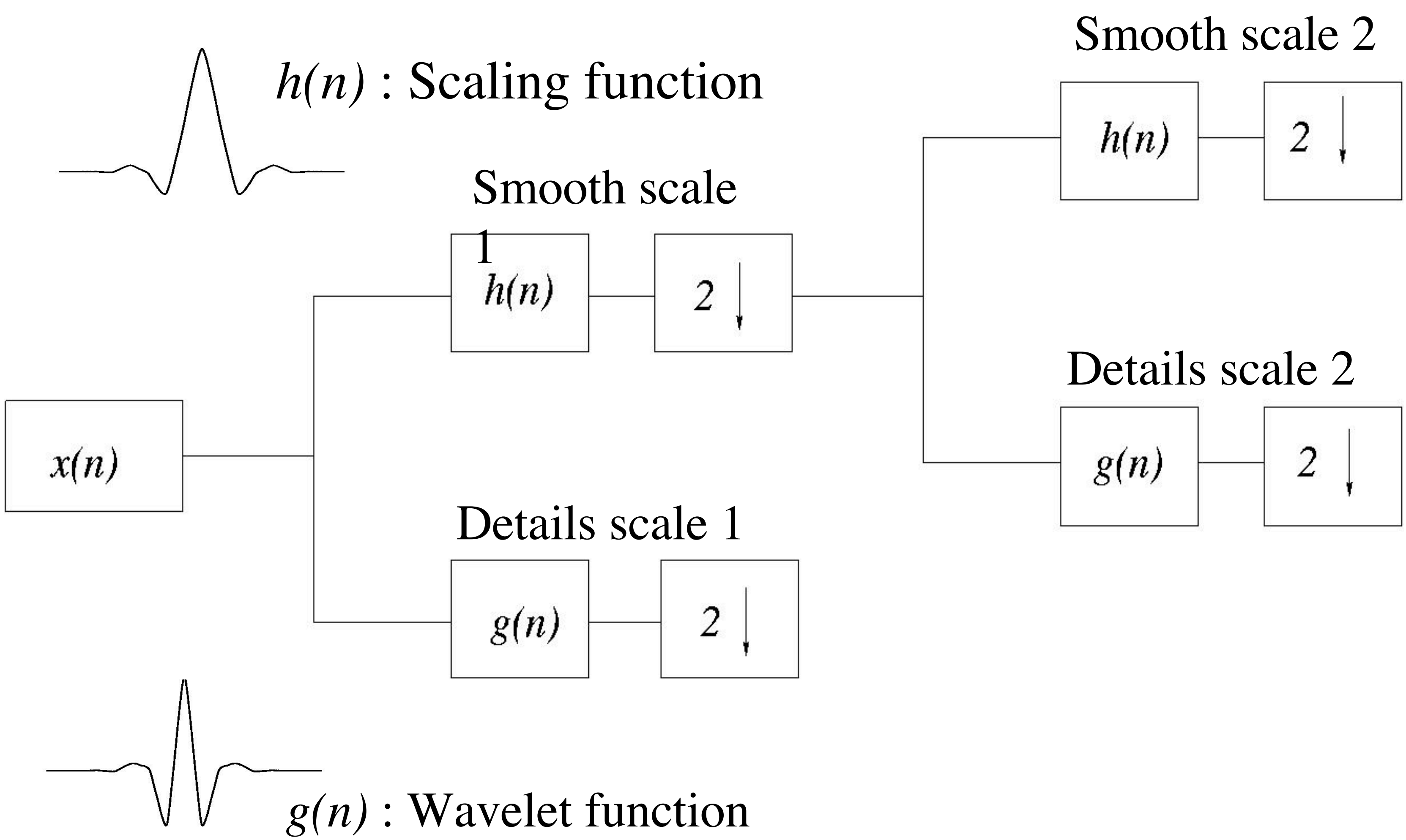

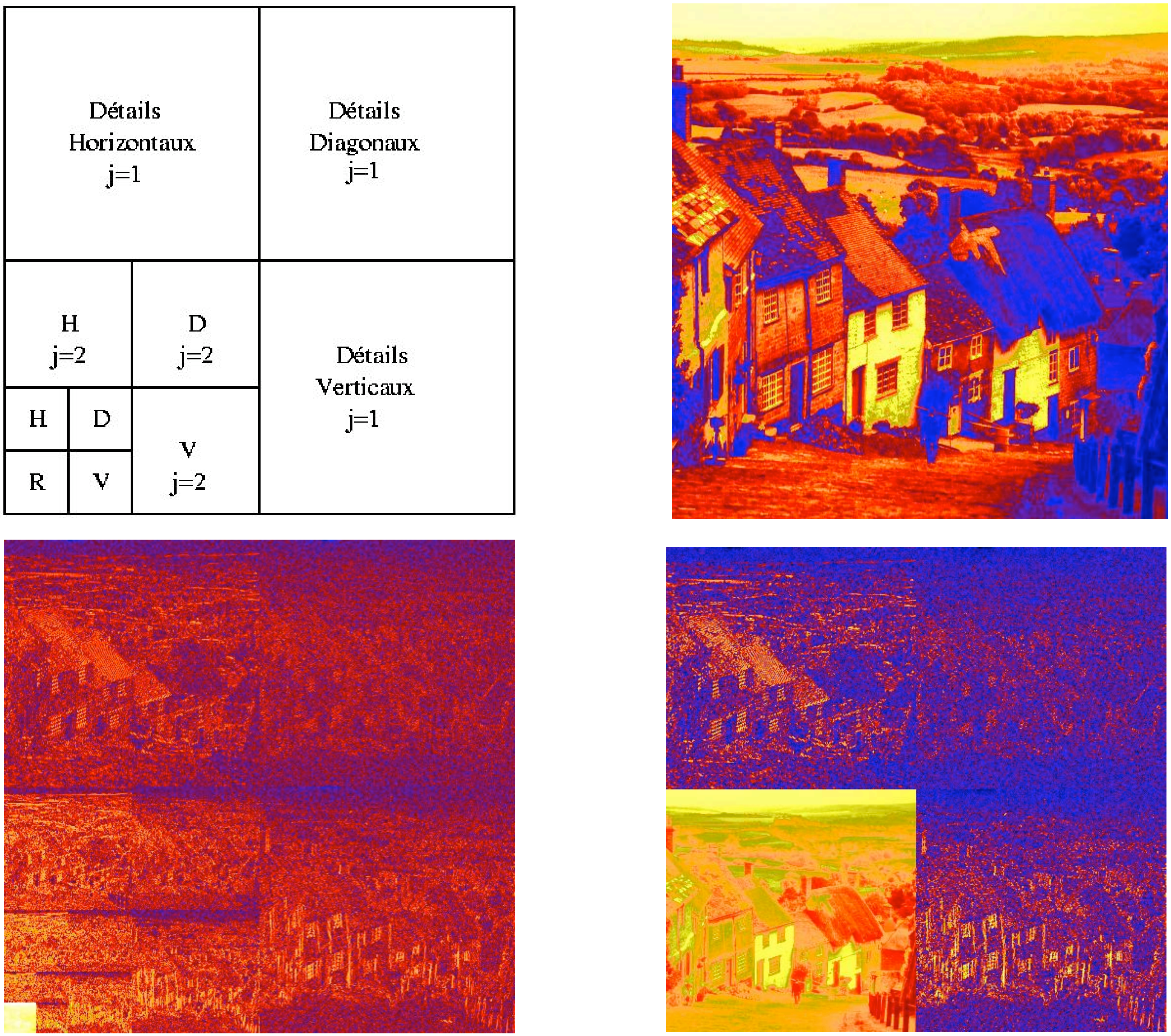

Détails
Horizontaux
j=1
Détails
Diagonaux
j=1
H
j=2
D
j=2
Détails
Verticaux
j=1
H
D
R
V
V
j=2

Statistical criteria

moments of the coefficient distribution

The Skewness

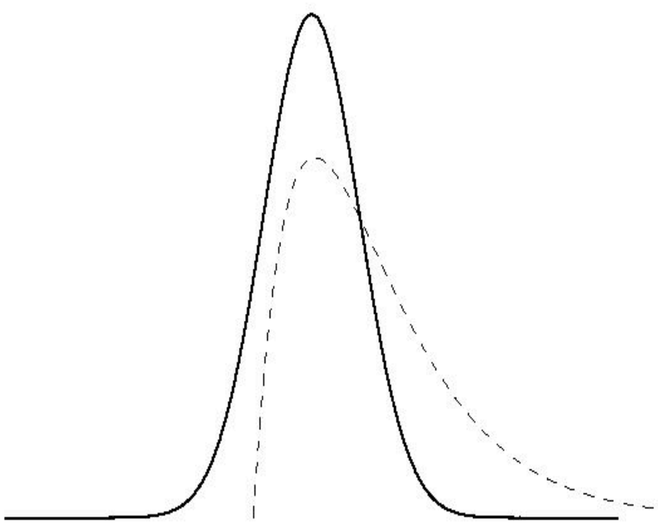

Disymmetry

The Kurtosis

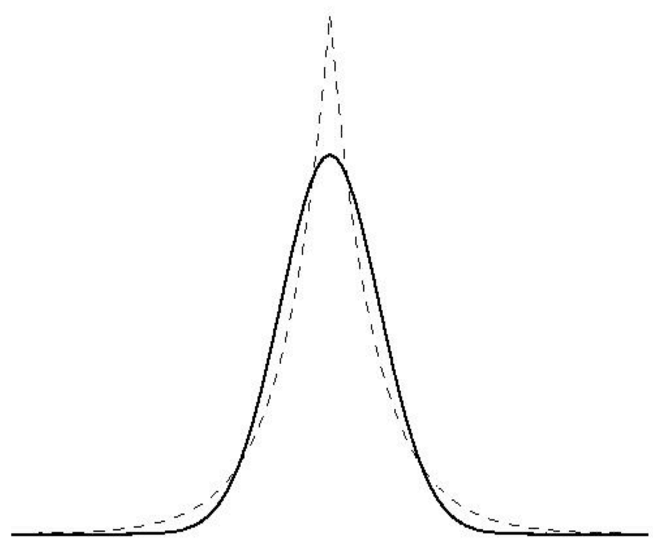

Flatness

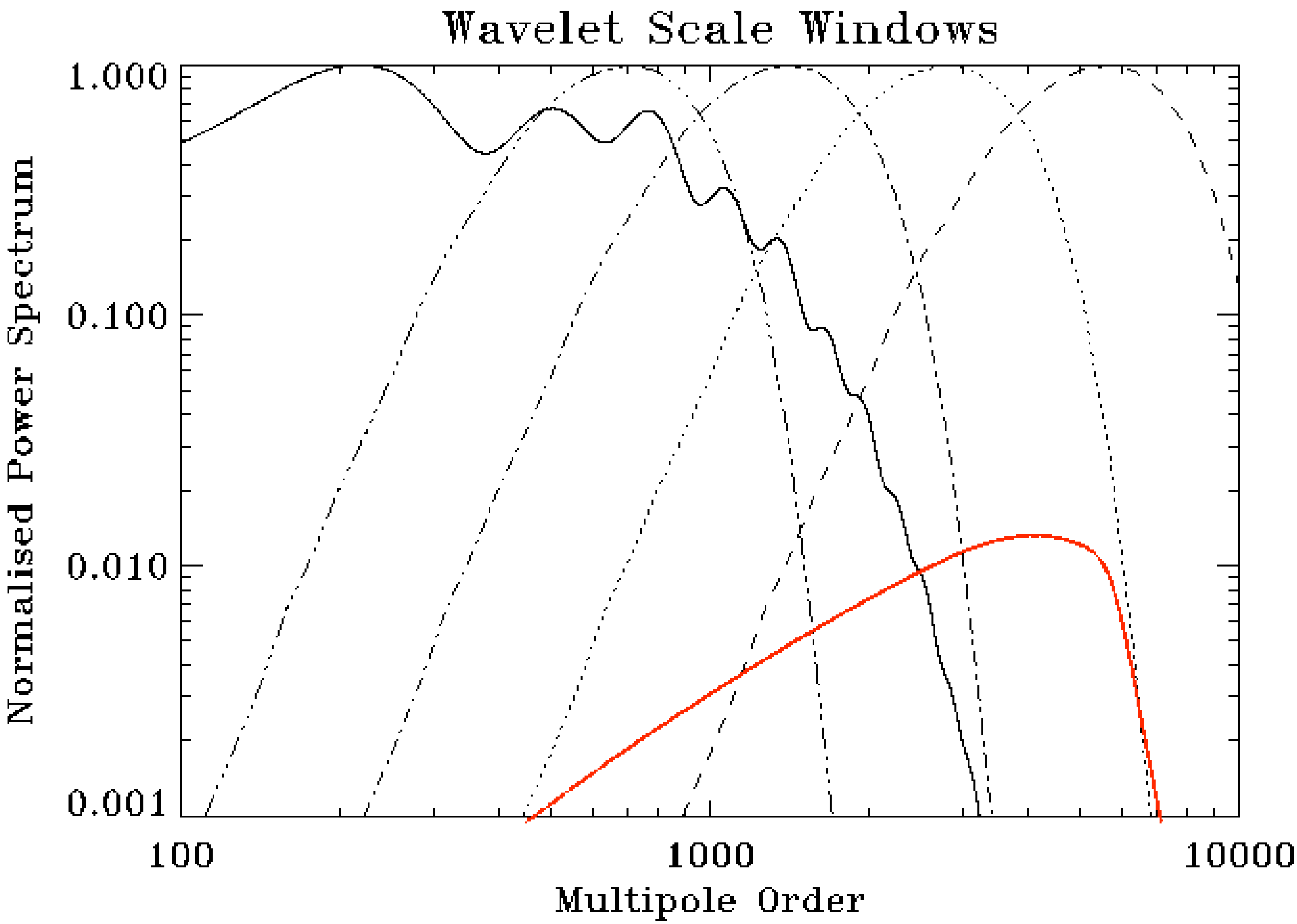
Wavelet Scale Windows
1.000
0.100
0.010
0.001
Normalised Power Spectrum
100
1000
10000
Multipole Order

Results

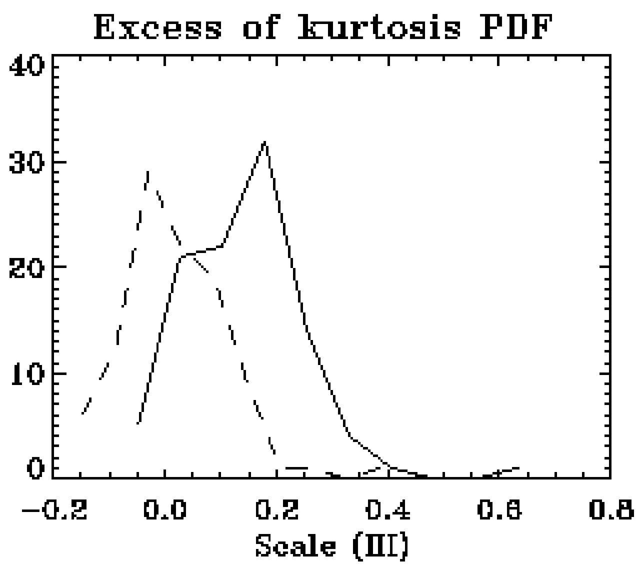

Diagonal details

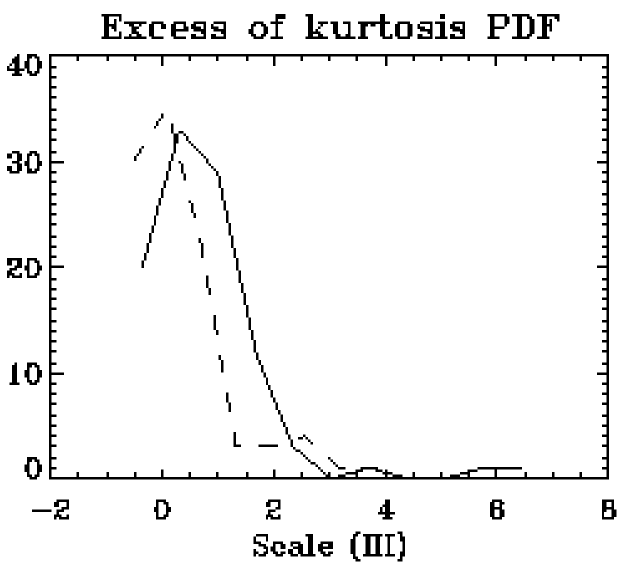

Gradient details

• The non-Gaussian character is detected to the third scale where the Gaussian signal dominates by a factor of 10.

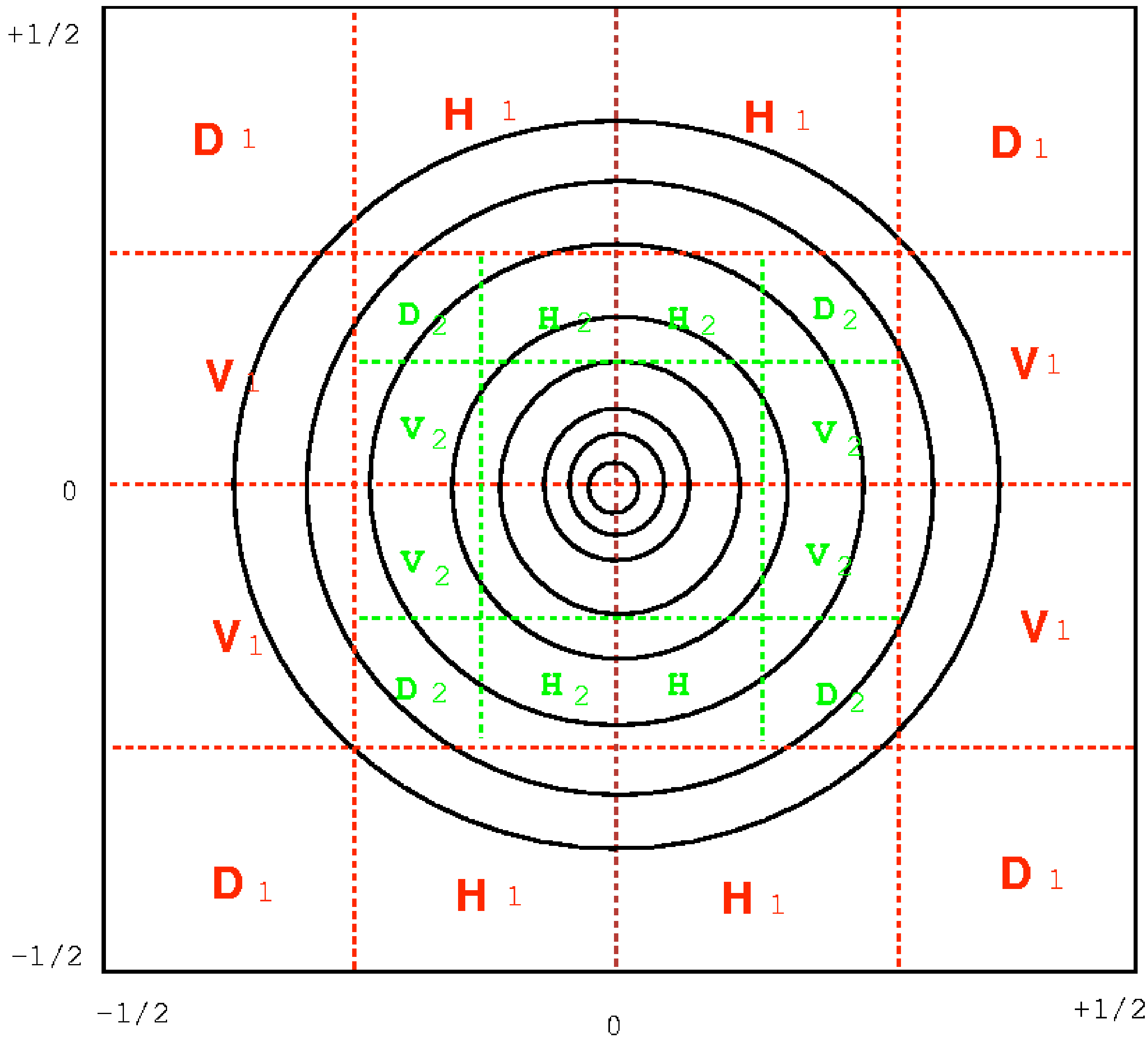

+1/2
0
-1/2
-1/2
0
+1/2
D 1
H 1
H 1
D 1
V 1
V 1
V 1
V 1
D 1
H 1
H 1
D 1
D 2
H 2
H 2
D 2
V 2
V 2
V 2
V 2
D 2
H 2
H
D 2

Comparison with other methods

- We have compared the bi-orthogonal transform with 3 and 4 point correlation functions.
- We have done this comparison on different simulated maps type (Point sources, filaments, etc…)
- We have also studied a very weak non-Gaussian process which results from the addition to a Gaussian field of a weak non-linear coupling of that field.

$$\chi(x) = \chi_G(x) + f_{NL}\,(\chi^2_G(x) - <\chi^2_G(x)>) \text{ with } f_{NL} = 0.01$$

- This kind of coupling can arise during the Inflation period.

Comparison with other methods

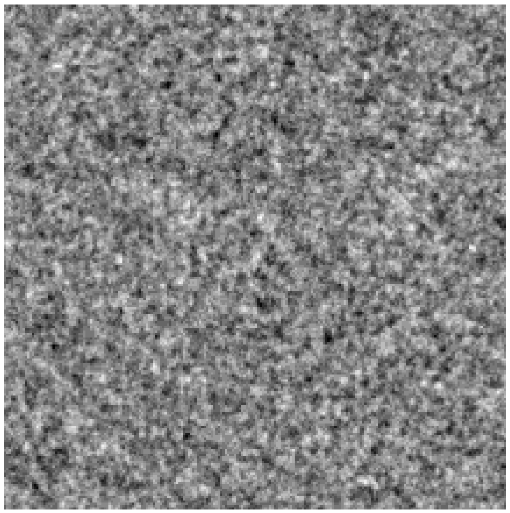

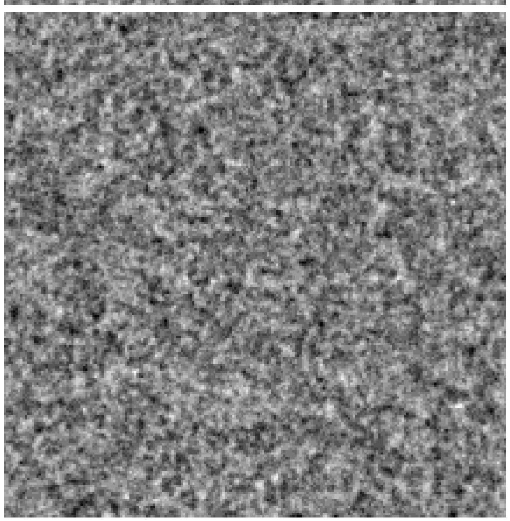

	Scale 1	Scale 2	Scale 3	Scale 4	Scale 5	Scale 6
Vertical	$2.08\ 10^{-18}$	0.226	0.488	0.828	0.158	0.368
G vs G	0.411	0.450	0.160	0.160	0.791	0.036
	0.488	0.426	0.367	0.426	0.426	0.189
G vs G	0.332	0.791	0.068	0.940	0.411	0.332
Horizontal	$1.97\ 10^{-17}$	0.002	0.828	0.555	0.695	0.625
G vs G	0.876	0.207	0.940	0.876	0.940	0.332
	0.315	0.0450	0.625	0.764	0.426	0.226
G vs G	0.264	0.596	0.411	0.940	0.596	0.791
Diagonal	0.001	0.157	0.828	0.368	0.315	0.315
G vs G	0.791	0.596	0.940	0.695	0.049	0.791
	0.828	0.695	0.930	0.828	0.764	0.963
G vs G	0.265	0.265	0.876	0.791	0.499	0.596

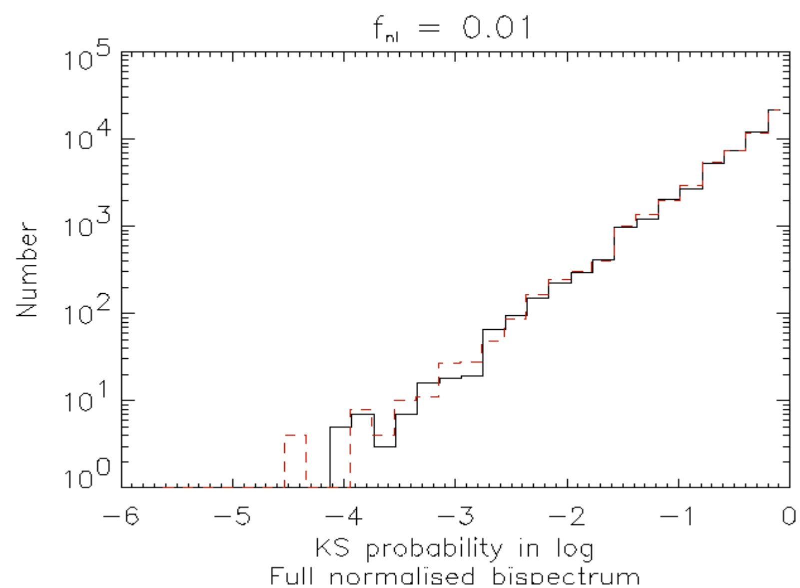

Conclusions

- The multiscale analysis is a very sensitive method to detect non-Gaussian signals.
- It is fast and demands low computing resources
- High order correlation function can be analytically predicted
- They can be directly related to physical phenomena.

Can we discriminate ?

- Primary fluctuations
  - Gaussian field resulting from inflation
  - Cosmic strings
- Secondary fluctuations
  - Kinetic SZ

3 types of simulation

- $\alpha^{1/2}$ CMB + $(1-\alpha)^{1/2}$ CS ($\alpha = 0.82$)
- CMB + Kinetic SZ
- $\alpha^{1/2}$ CMB + $(1-\alpha)^{1/2}$ CS + Kinetic SZ

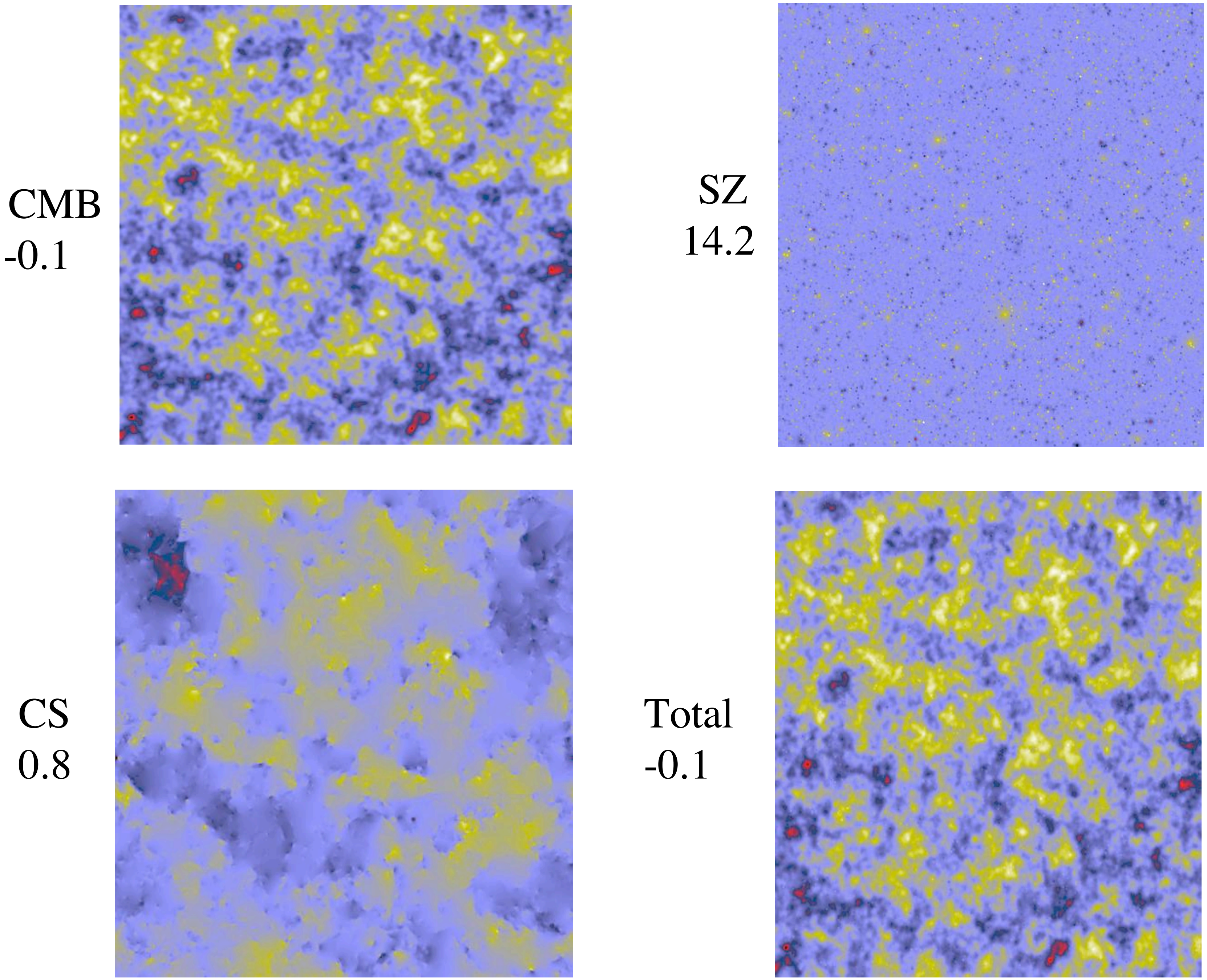
CMB
-0.1
SZ
14.2
CS
0.8
Total
-0.1

Multiscale Analysis

We have applied the following transforms.

- bi-orthogonal wavelet transform
- undecimated isotropic wavelet transform
- Ridgelets transform with 16 pixels aside sub-images
- Ridgelets transform with 32 pixels aside sub-images
- Curvelets

Undecimated isotropic wavelet transform

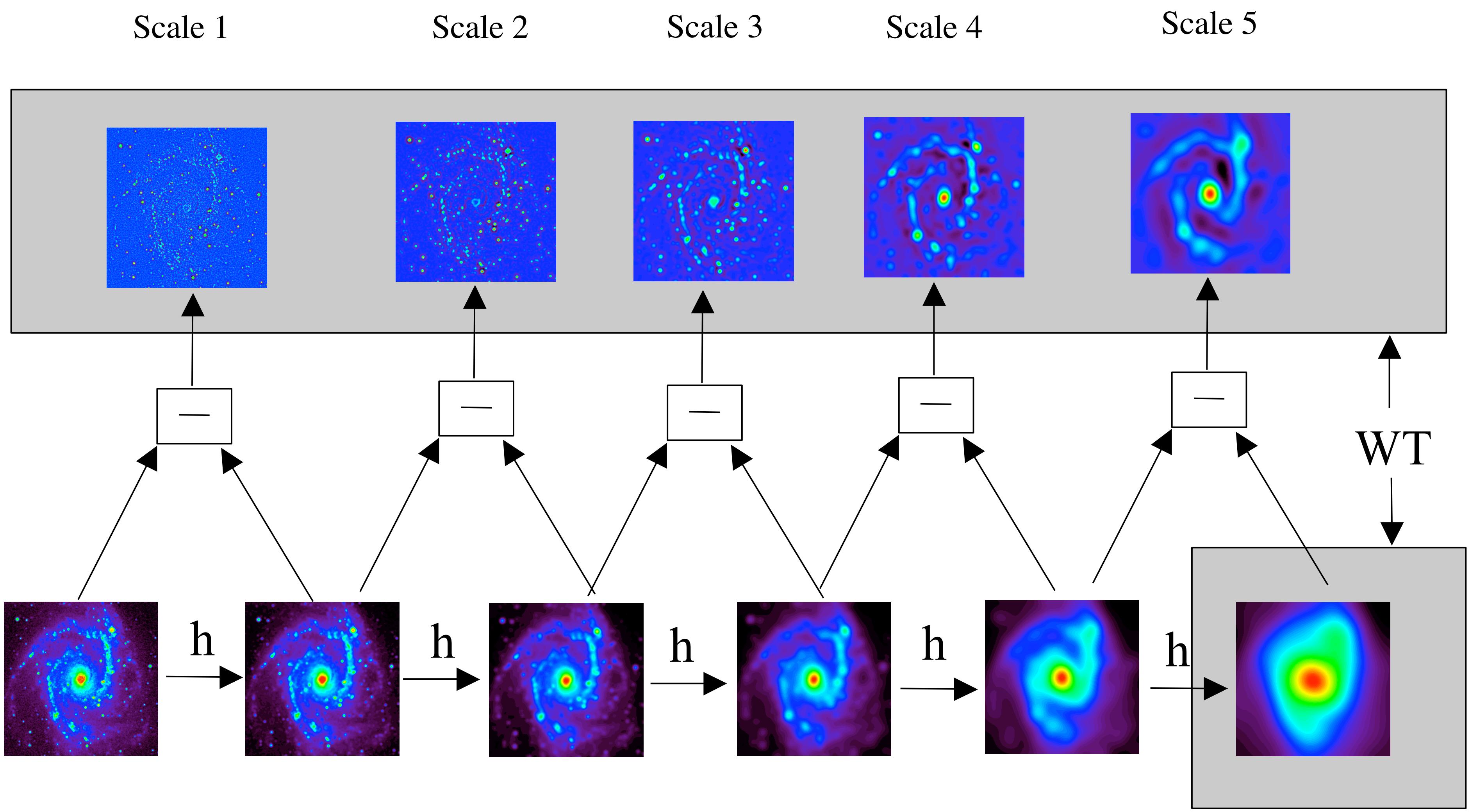

$$I(x,y) = c_J(x,y) + \sum_{j=1}^{J} w(j,x,y)$$

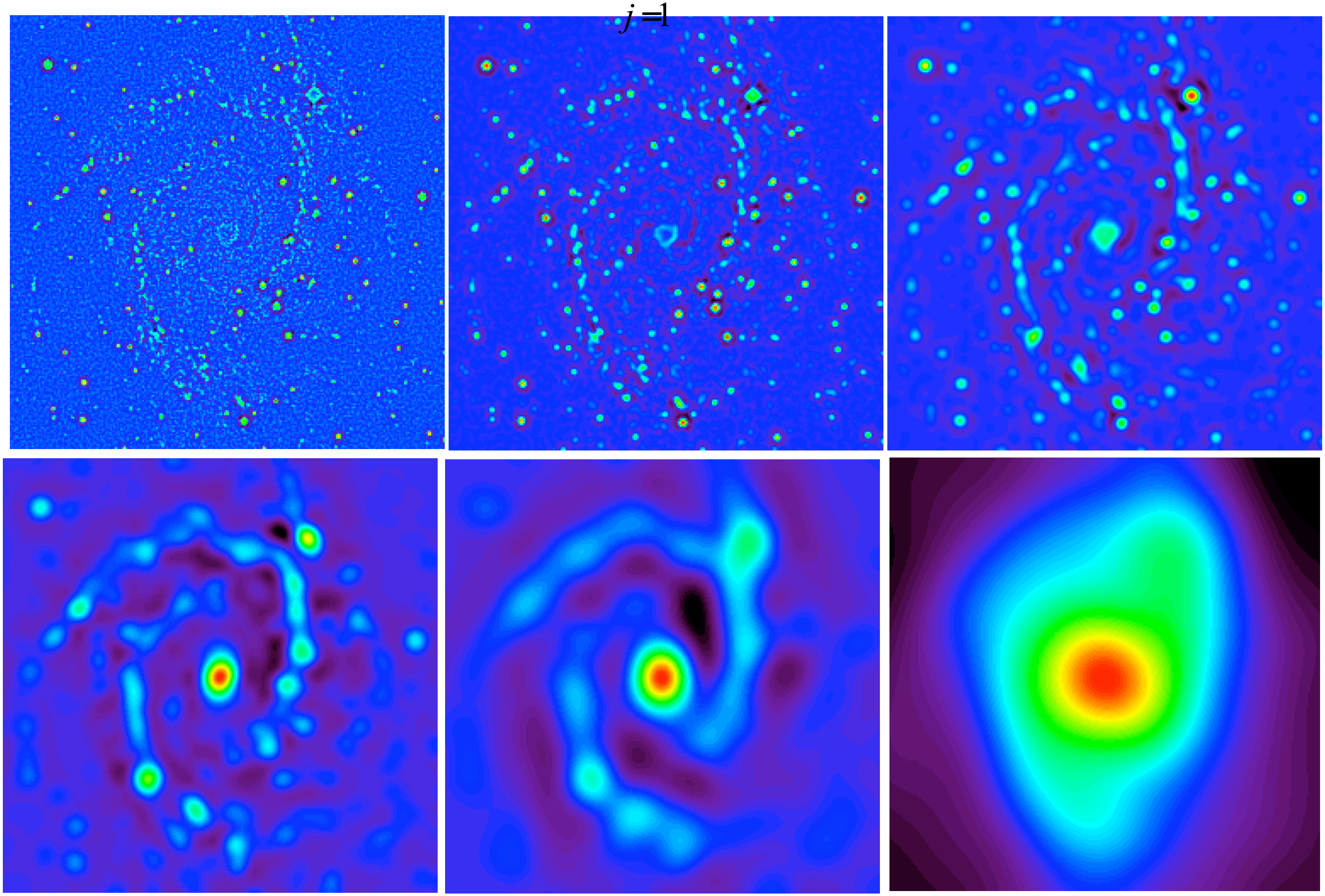

Ridgelet Transform

Ridgelet Transform (Candes, 1998), with ridgelet function below:

$$\psi_{a,b,\vartheta}(x) = a^{1/2}\psi\left(\frac{\left(x_1\cos(\vartheta) + x_2\sin(\vartheta) - b\right)}{a}\right)$$

The function is constant along lines. Transverse to this ridge, it is a wavelet.

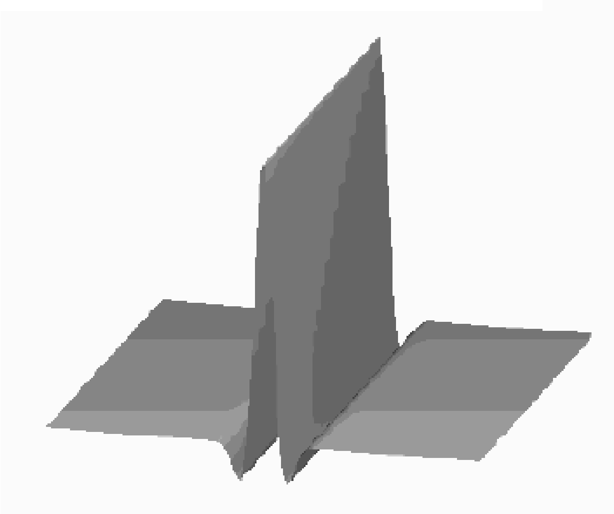

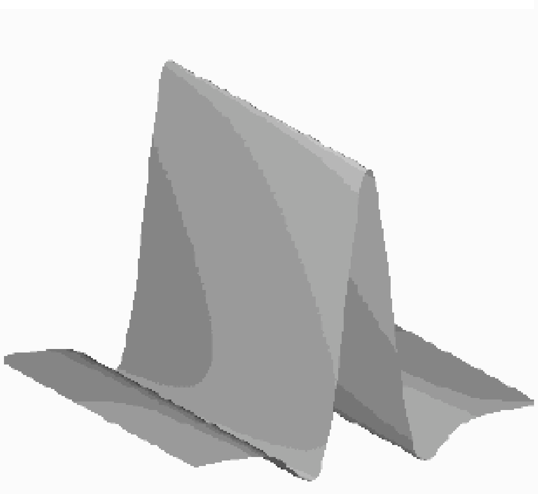

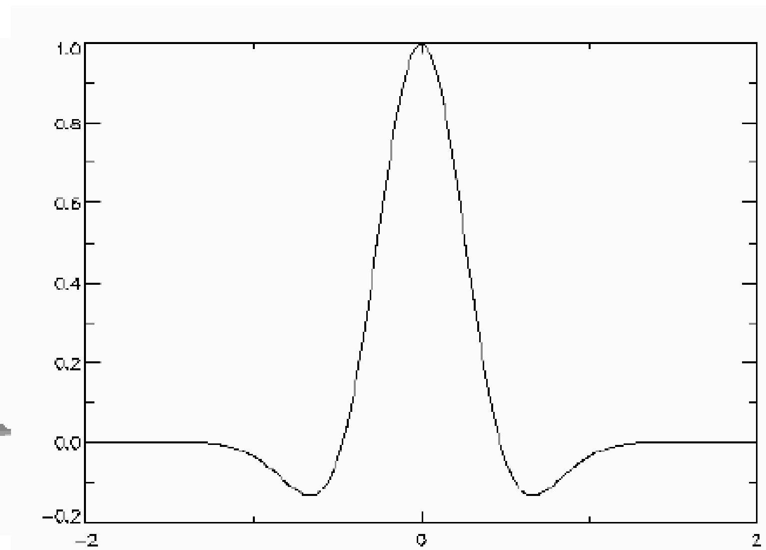

The Curvelet Transform

The curvelet transform (Candes & Donoho. 1999) is a combination of reversible transformations:

- à trous 2D isotropic wavelet transform
- partitionning
- ridgelet transform

Samples curved features in optimal numbers of linear structures of different sizes.

Less coefficients are needed in the curvelet transform

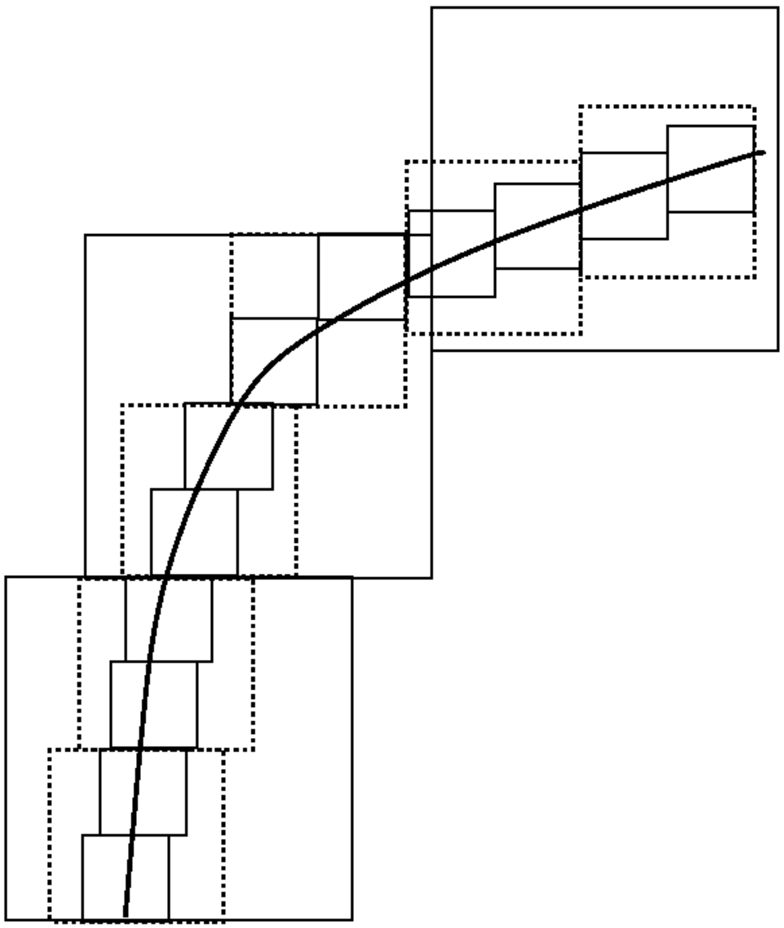

Wavelet transform

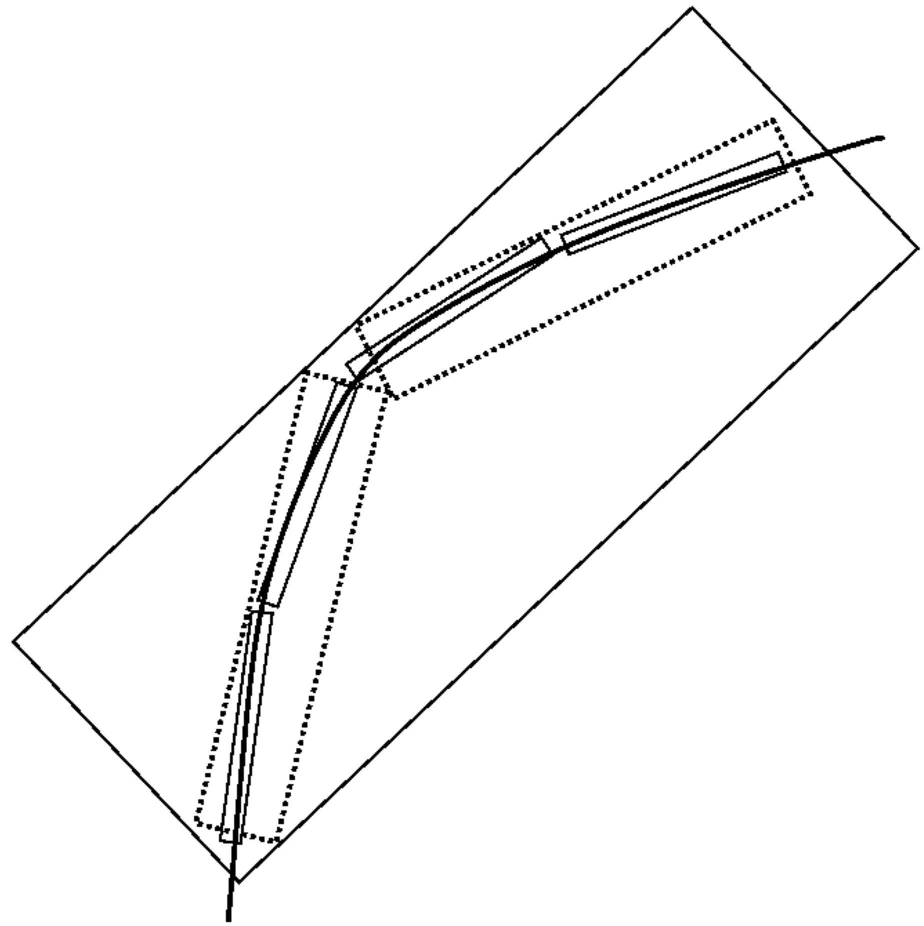

Curvelet transform

Curvelet transform of a circle at 2 scales

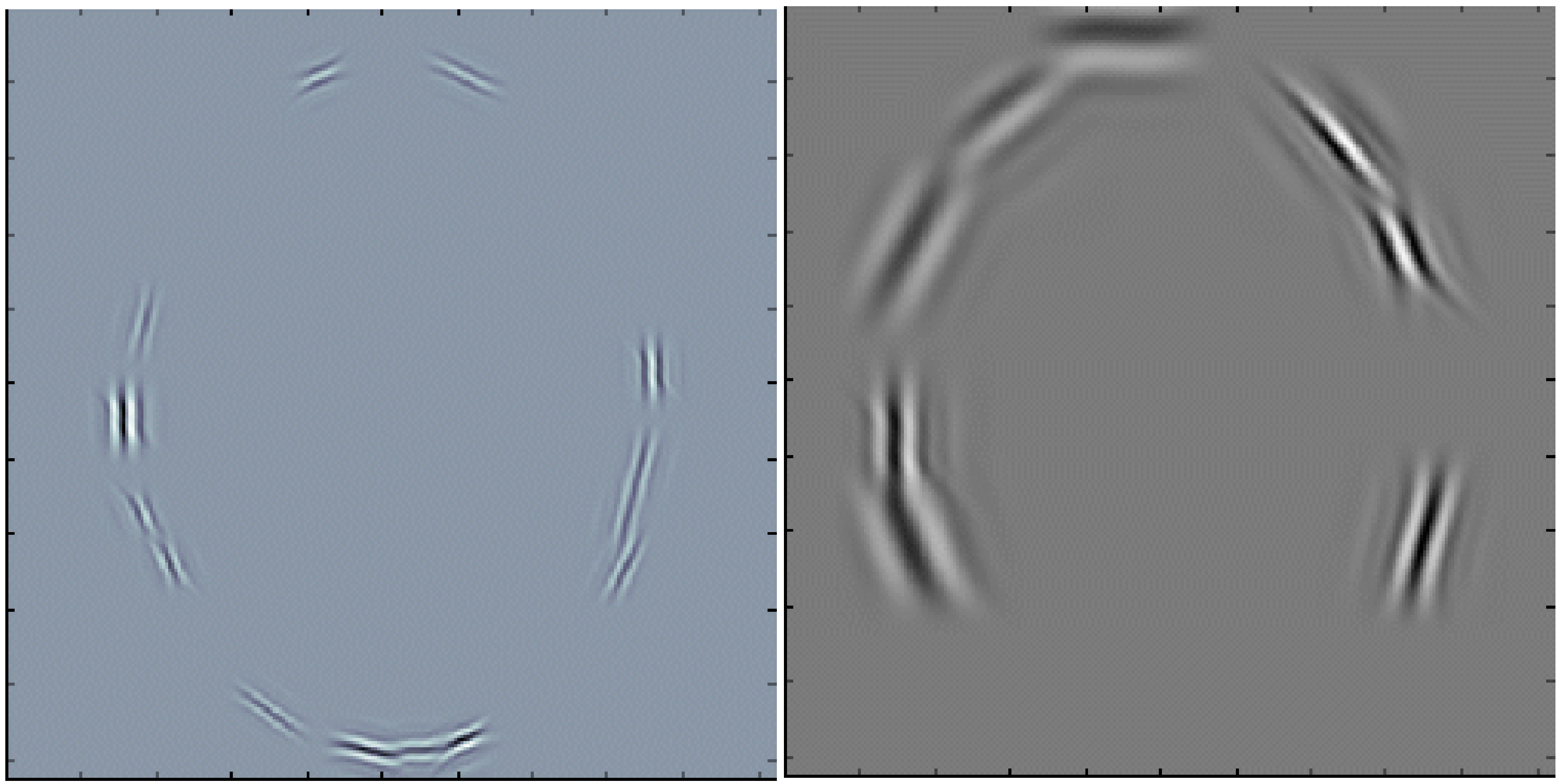

Multiscale Analysis of the CMB

- Isotropic wavelet transform
- Bi-orthogonal wavelet transform
- Curvelet transform
- Ridgelet transform

Applied on simulated maps of secondary + primary anisotropies:

1) **CMB + KSZ** 2) **CMB + CS** 3) **CMB + KSZ + CS**

The Gaussian realisations with the same power spectra.

We compare the normalised excess kurtosis values

Results @scale 1 (3')

	Bi-orth.	A trous	Ridgelet	Curvelet
CMB+KSZ	1106.	65.	0.1	10.
CMB+CS	1813.	424.	5.7	198.
CMB+CS+KSZ	1040.	392.	5.9	165.

Results @scale 2 (6')

	Bi-orth.	A trous	Ridgelet	Curvelet
CMB+KSZ	47.	1.	0.1	0.2
CMB+CS	261.	11.	0.7	8.
CMB+CS+KSZ	196.	12.	0.8	7.

Conclusions

- Bi-orthogonal wavelets are always the most sensitive tool.

- Ridgelet and curvelet transforms are sensitive to CS only.

- In a mixture CS+KSZ dominated by a Gaussian field:
  isotropic bi-orthogonal wavelets detect non-Gaussianity
  anisotropic curvelets and ridgelets discriminate CS from KSZ.

Can we separate ?

- Thermal SZ
  - Spectral signature => Compton parameter
- Kinetic SZ
  - No spectral signature
  - Cannot be separated from primordial fluctuations

Can we separate KSZ ?

Hypotheses

2 processes : CMB + SZ

Component separation

Temperature fluctuation : CMB+KSZ

Compton parameter : TSZ

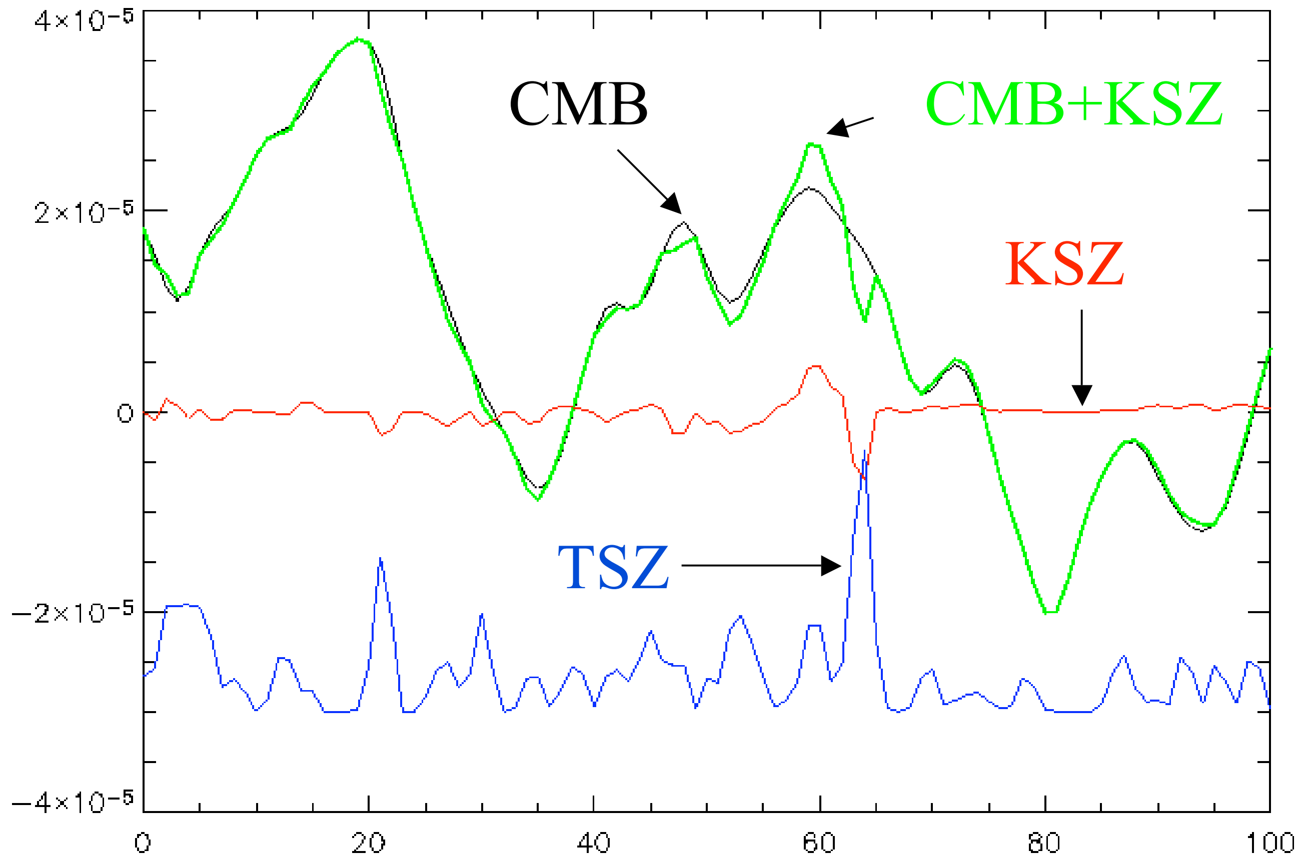

CMB
CMB+KSZ
KSZ
TSZ
4×10⁻⁵
2×10⁻⁵
0
−2×10⁻⁵
−4×10⁻⁵
0
20
40
60
80
100

Spatial correlation between TSZ and KSZ

- if not TSZ then CMB
- if TSZ then CMB+KSZ

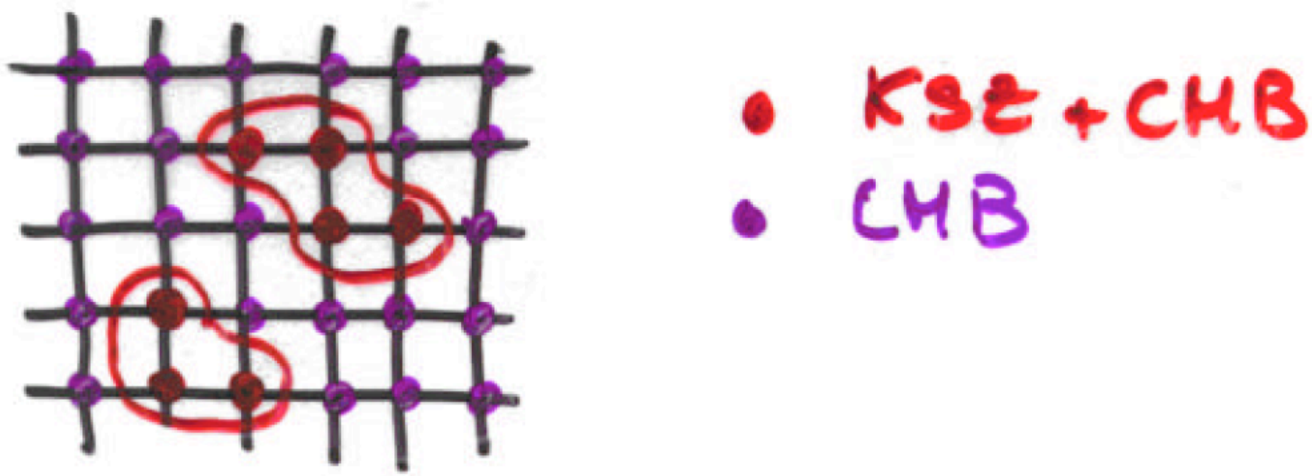

Interpolation

$$\boldsymbol{f}_w = \boldsymbol{W}\boldsymbol{u} + \lambda \boldsymbol{L}\boldsymbol{u} = \boldsymbol{A}\boldsymbol{u}$$

$\boldsymbol{W}$: weight matrix

When w=0 then Lu=0 (unknown points)
w=1 then f=u + λ Lu (known points)

λ controls the tightness of the fit
=> small λ then f=u

TSZ is used as a spatial template

Use of a complete set of thresholds gives a set of estimated KSZ

Minimization

Identify criteria that distinguish CMB from KSZ

1. KSZ dominates at high wavenumber
2. KSZ is non-Gaussian

=> Wavelet transform

- Diagonal details at the first scale
- TSZ spatially correlated coefficients

$$\zeta = \mathrm{Min}\left[\frac{(\mathcal{M}_2(w_0) - \mathcal{M}_2(w))^2}{\mathcal{M}_2^2(w_0)} + \frac{(\mathcal{M}_4(w_0) - \mathcal{M}_4(w))^2}{\mathcal{M}_4^2(w_0)}\right]$$

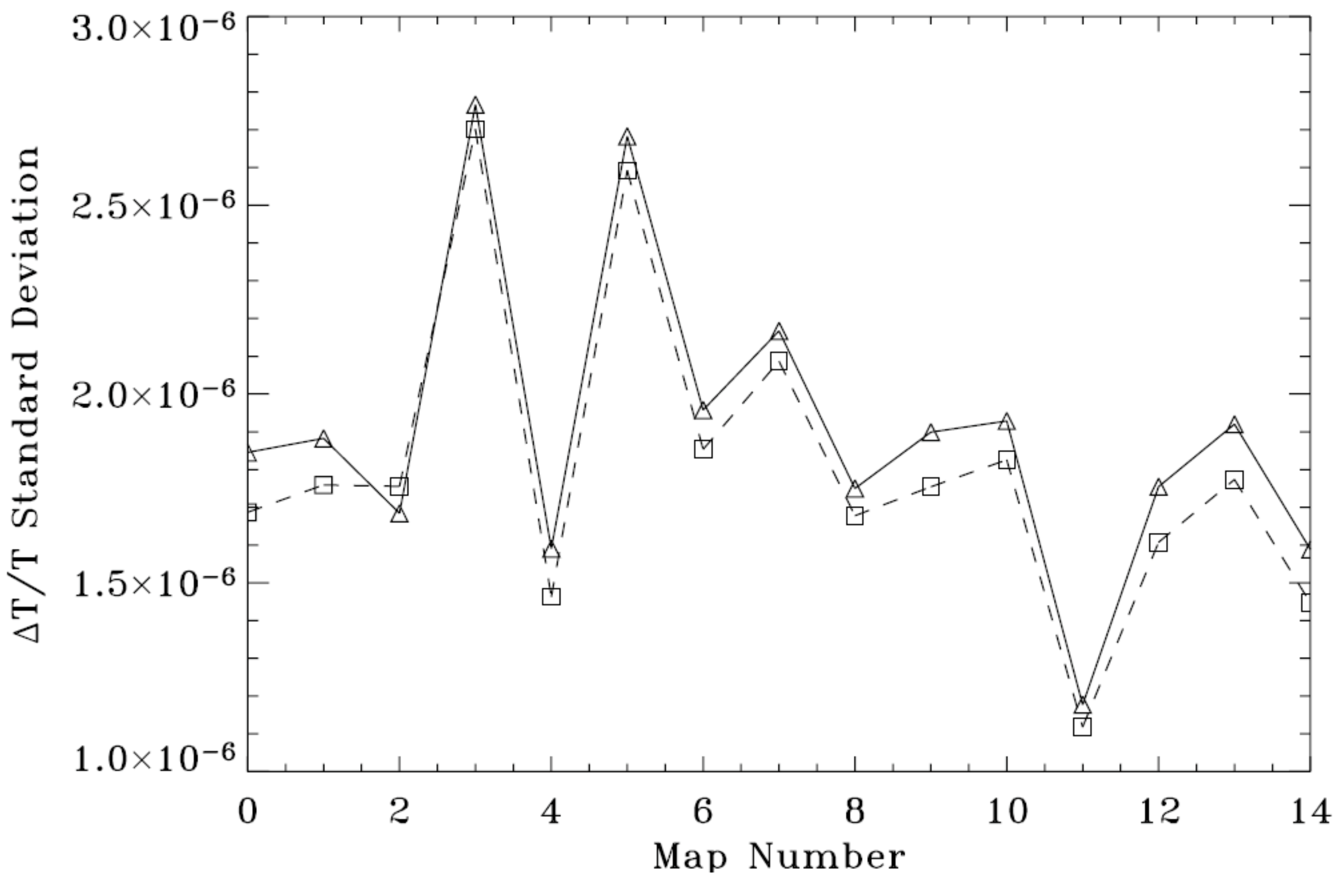

Mean correlation coefficient : 0.78

Mean error on σ : 5%

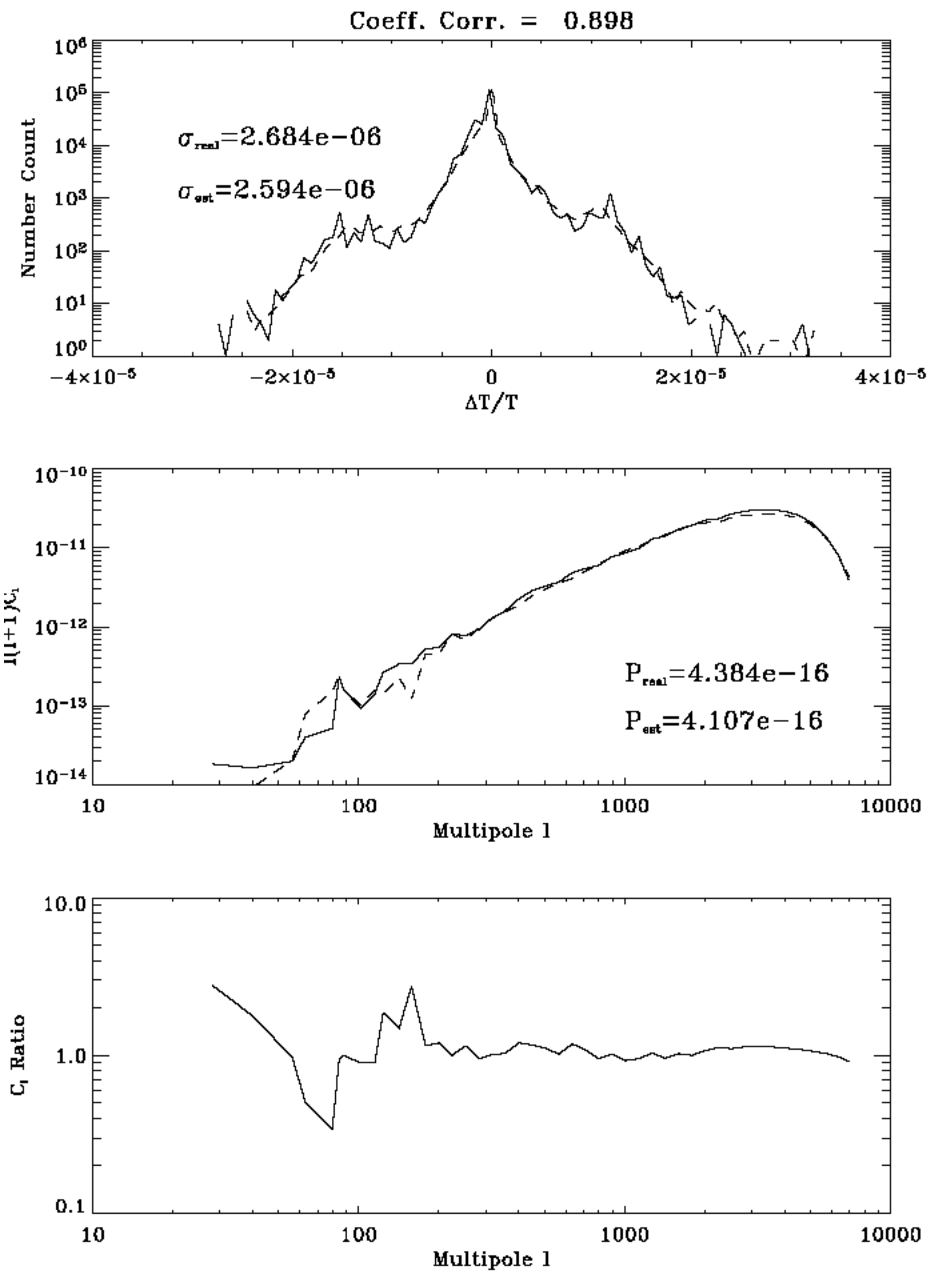

Coeff. Corr. = 0.898
Number Count
σ_real=2.684e−06
σ_est=2.594e−06
ΔT/T
l(l+1)C_l
P_real=4.384e−16
P_est=4.107e−16
Multipole l
C_l Ratio
Multipole l

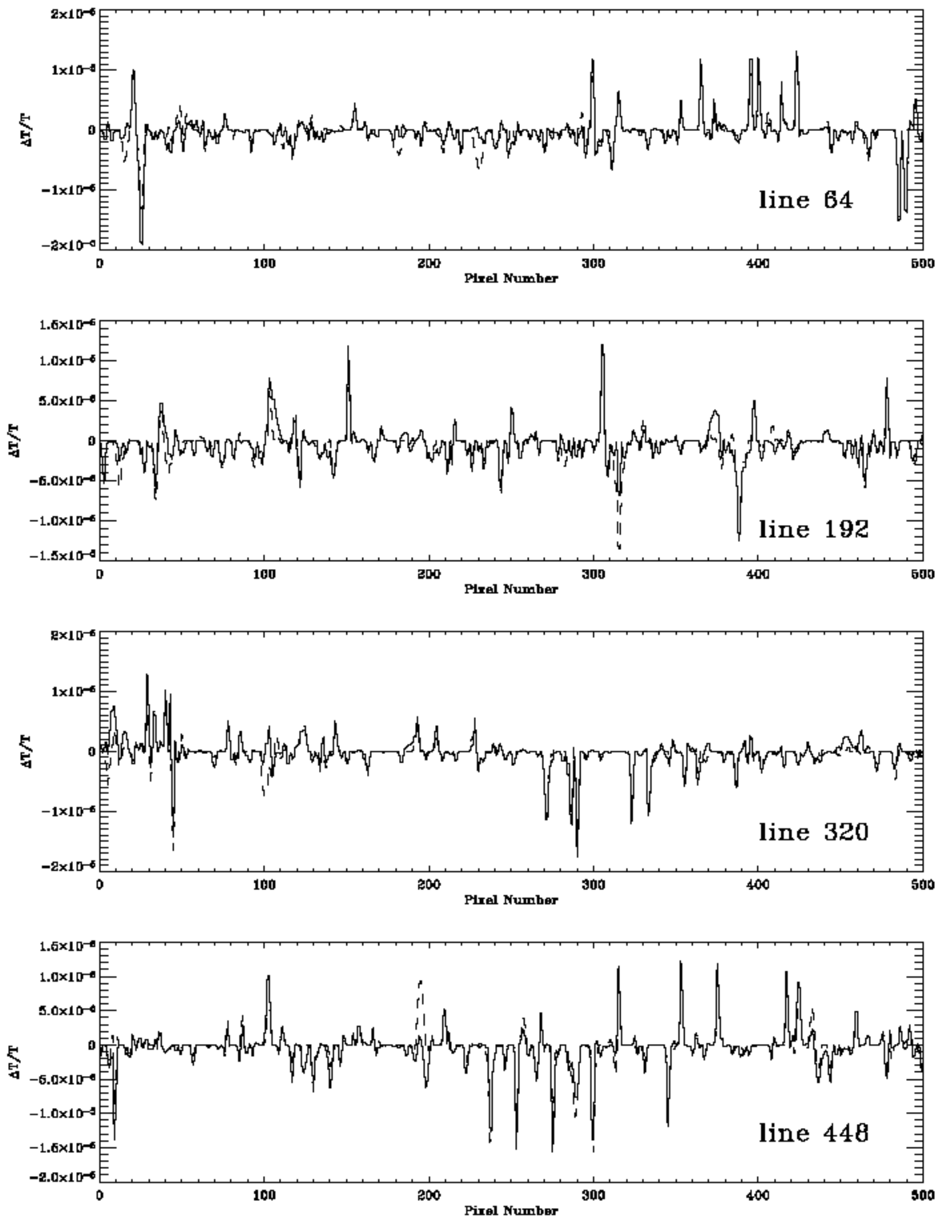

ΔT/T
Pixel Number
line 64
line 192
line 320
line 448
0
100
200
300
400
500

Conclusions

- Need of a spatial template
- Add the skewness to account for other components
- Add other wavelet scales to account for the noise and beam dilution

MARS EXPRESS

ORBIT:

- Orbital inclination : 86.3^{o}
- Pericentre: 258 km
- Apocentre: 11 560 km
- Period: 7.5 h

OMEGA

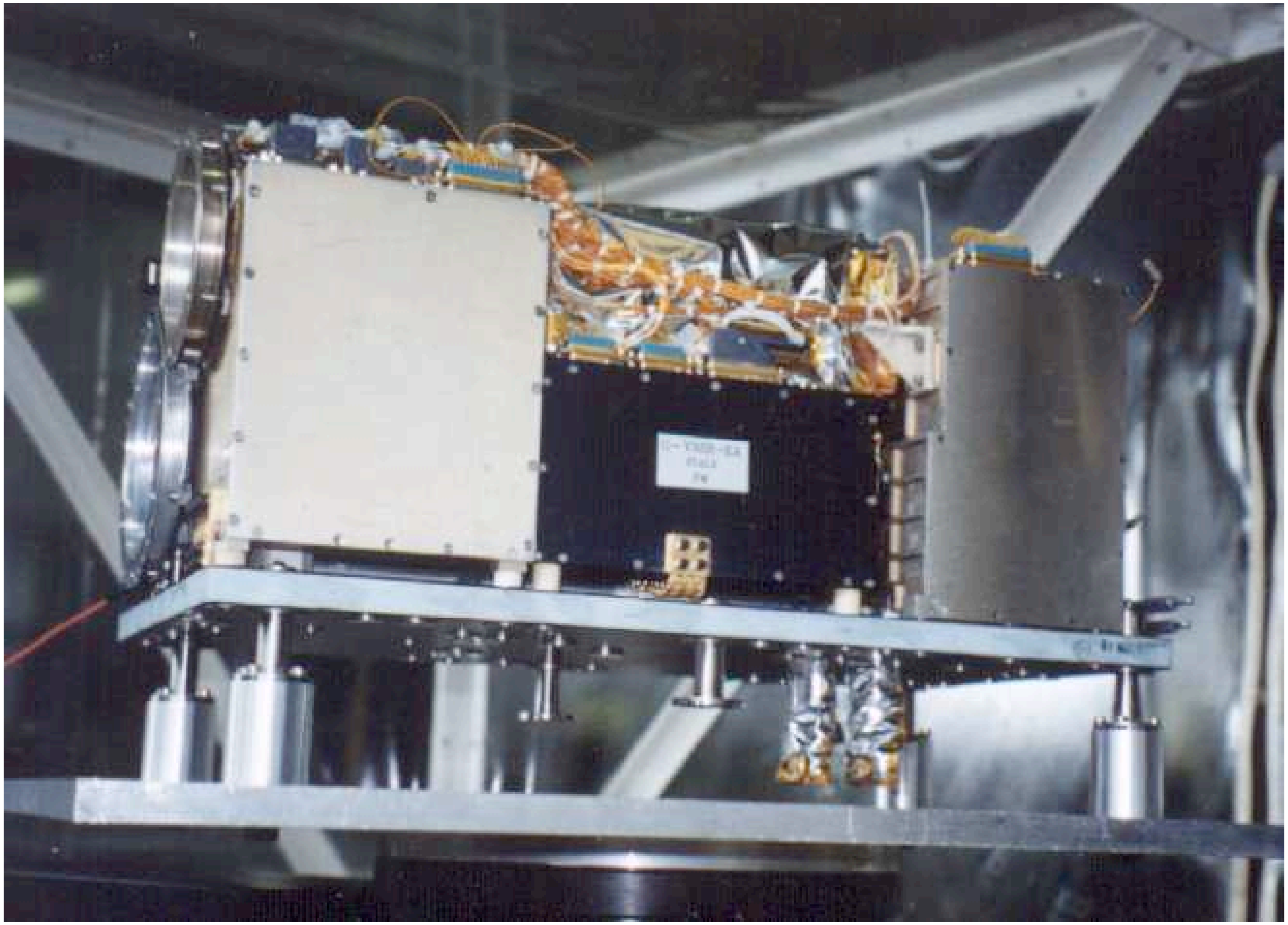

OMEGA

Visible – Infrared Spectrometre 0.36-5.1 µm

• IFOV : 4.1 arcmin

• Visible channel : CCD 384 x 288 pixels (spatial x spectral) : 0.36-1.1 µm

• Infrared channel : 2 linear InSb 128 pixels detectors cooled at 70 K.

0.93-2.7 µm et 2.5-5.1 µm with a spectral resolution of 13 and 20 nm

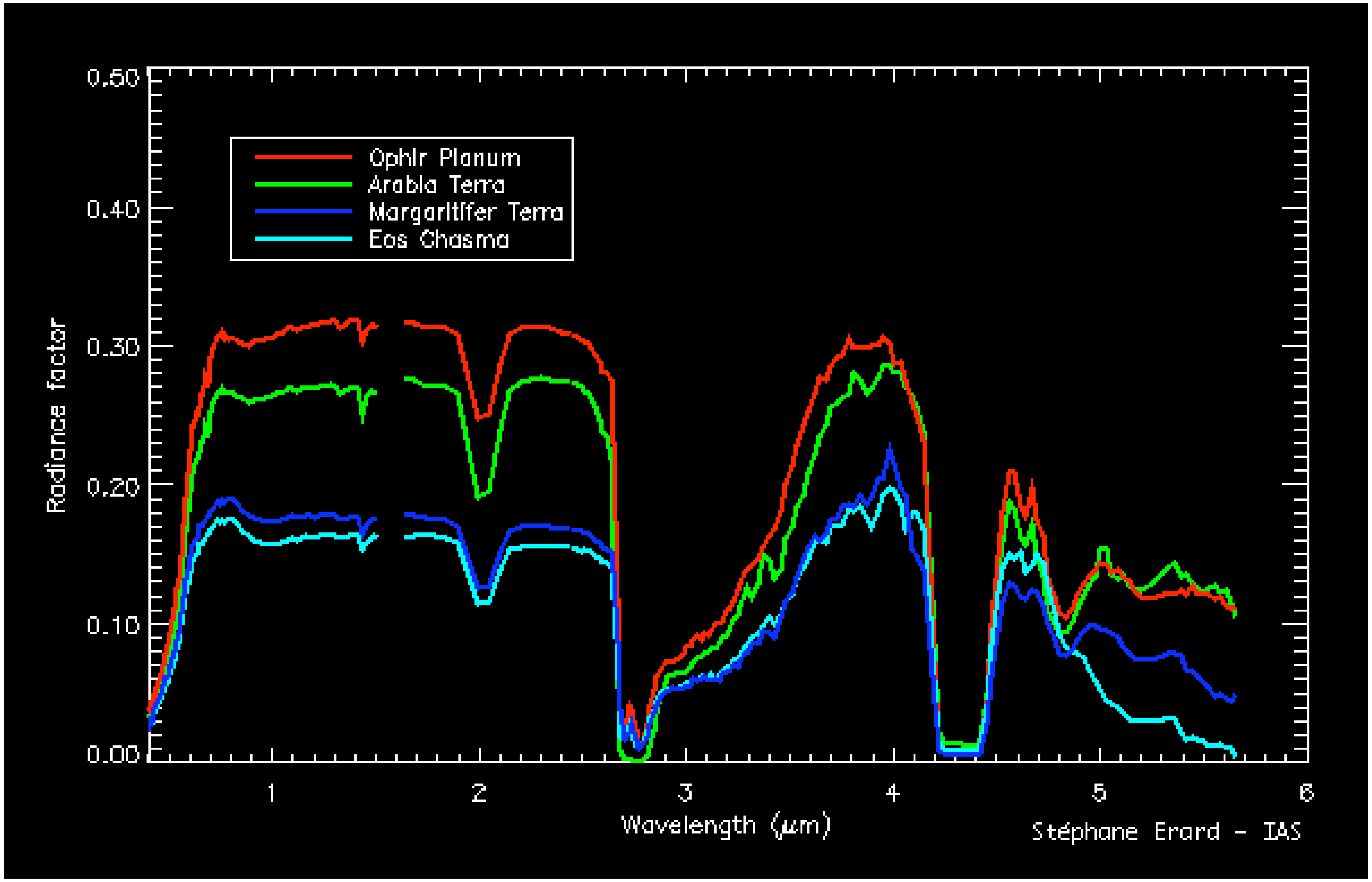

Ophir Planum
Arabia Terra
Margaritifer Terra
Eos Chasma
Radiance factor
0.50
0.40
0.30
0.20
0.10
0.00
1
2
3
4
5
6
Wavelength (μm)
Stéphane Erard - IAS

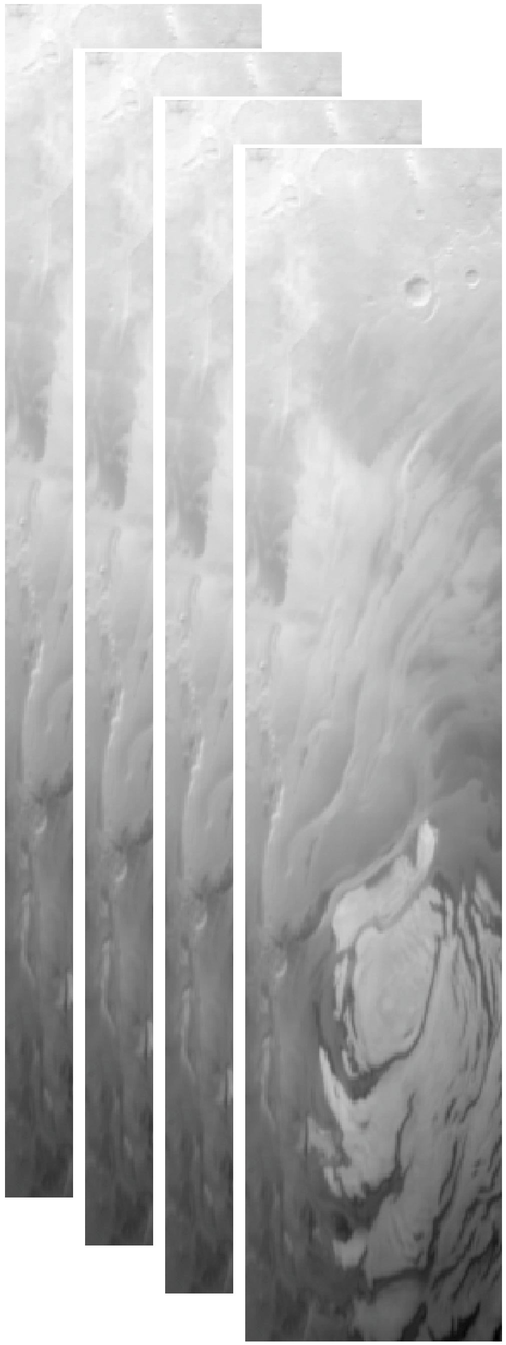

CUBE : 2 spatial directions (Nx x Ny samples) x 1 spectral direction (Nz sources)

Nc independent components given by ICA

- ICA is applied on the direct cube

- ICA is applied on the wavelet transformed cube

Independent Component Analysis

- What we observe (x) is a linear combination of independent *latent* variables (s_i)

$$x = a_1s_1 + a_2s_2 + \ldots + a_ns_n$$

- The independent variables have non-Gaussian probability distribution function

Independent Component Analysis

- We cannot determine the variances (energies) of the independent variables.
- We cannot determine the order of the independent variables.
- We cannot characterise Gaussian distributed variables.

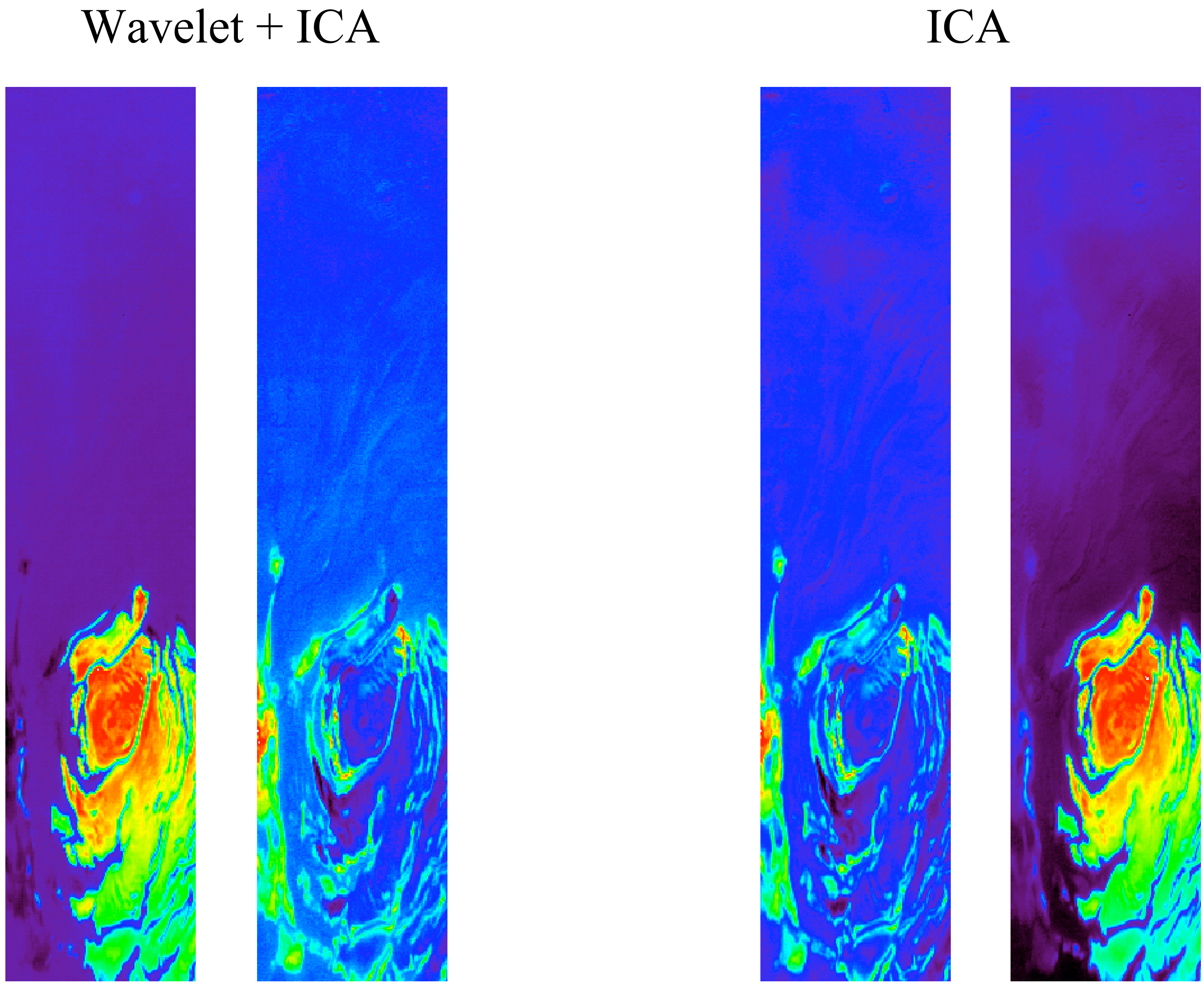

Wavelet + ICA
ICA

CO_2 Ice Component

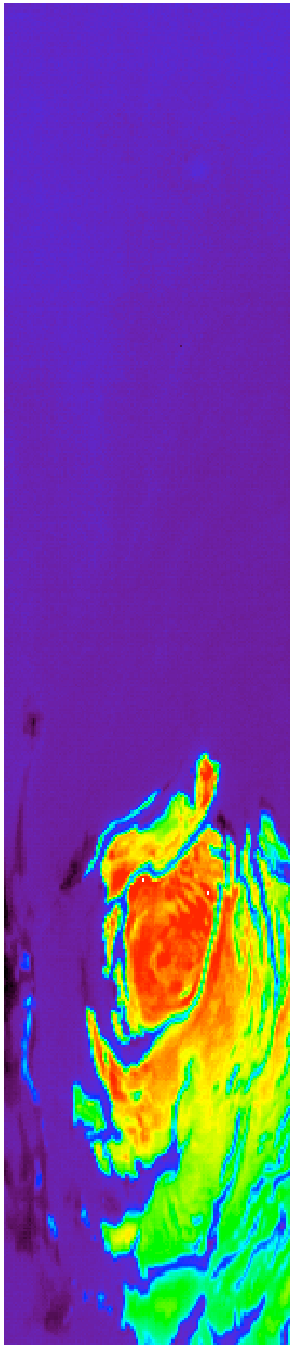

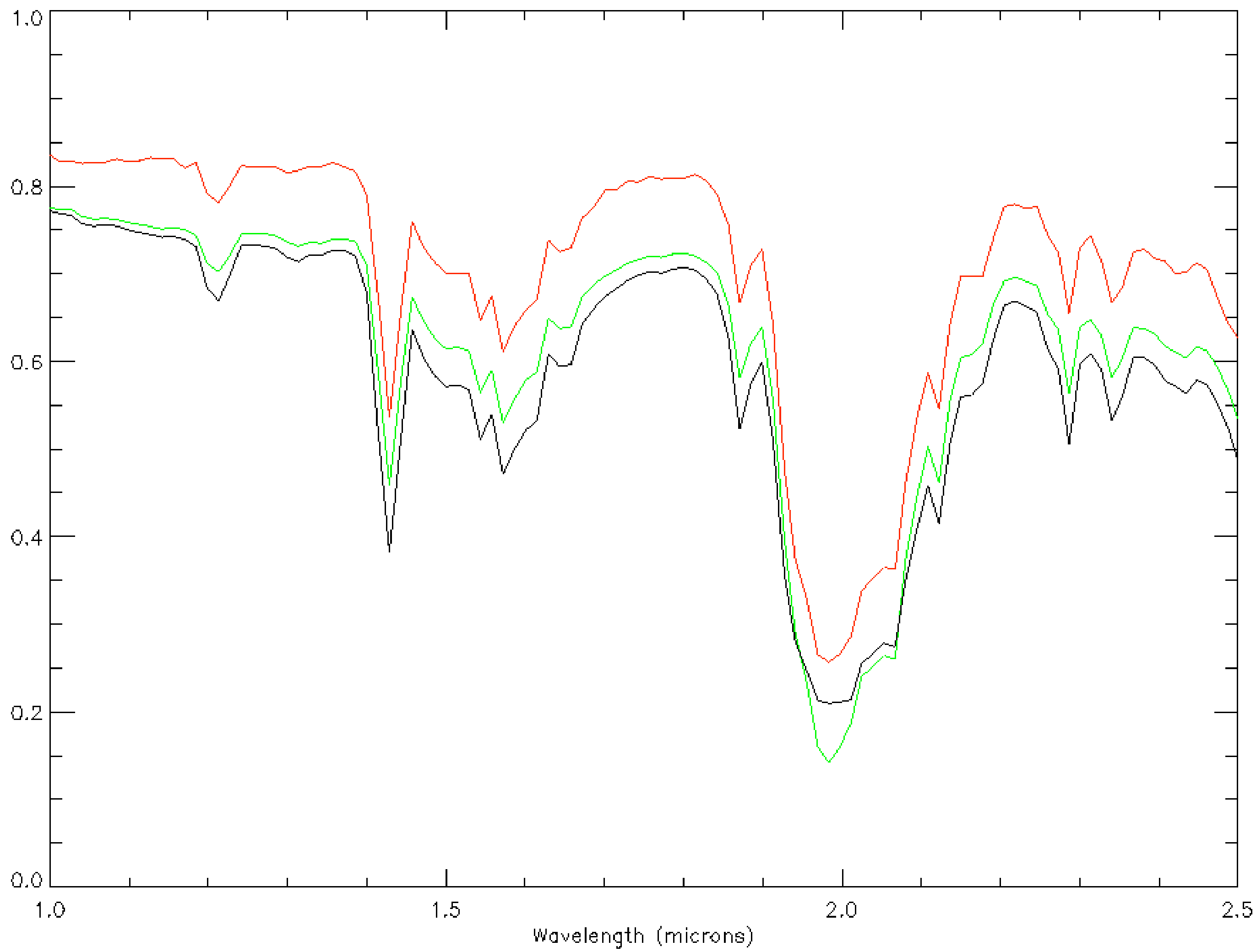

H_2O Ice Component

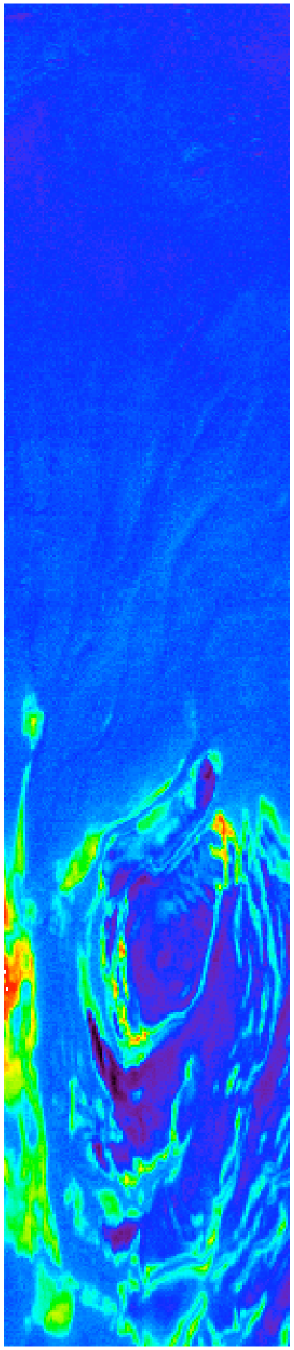

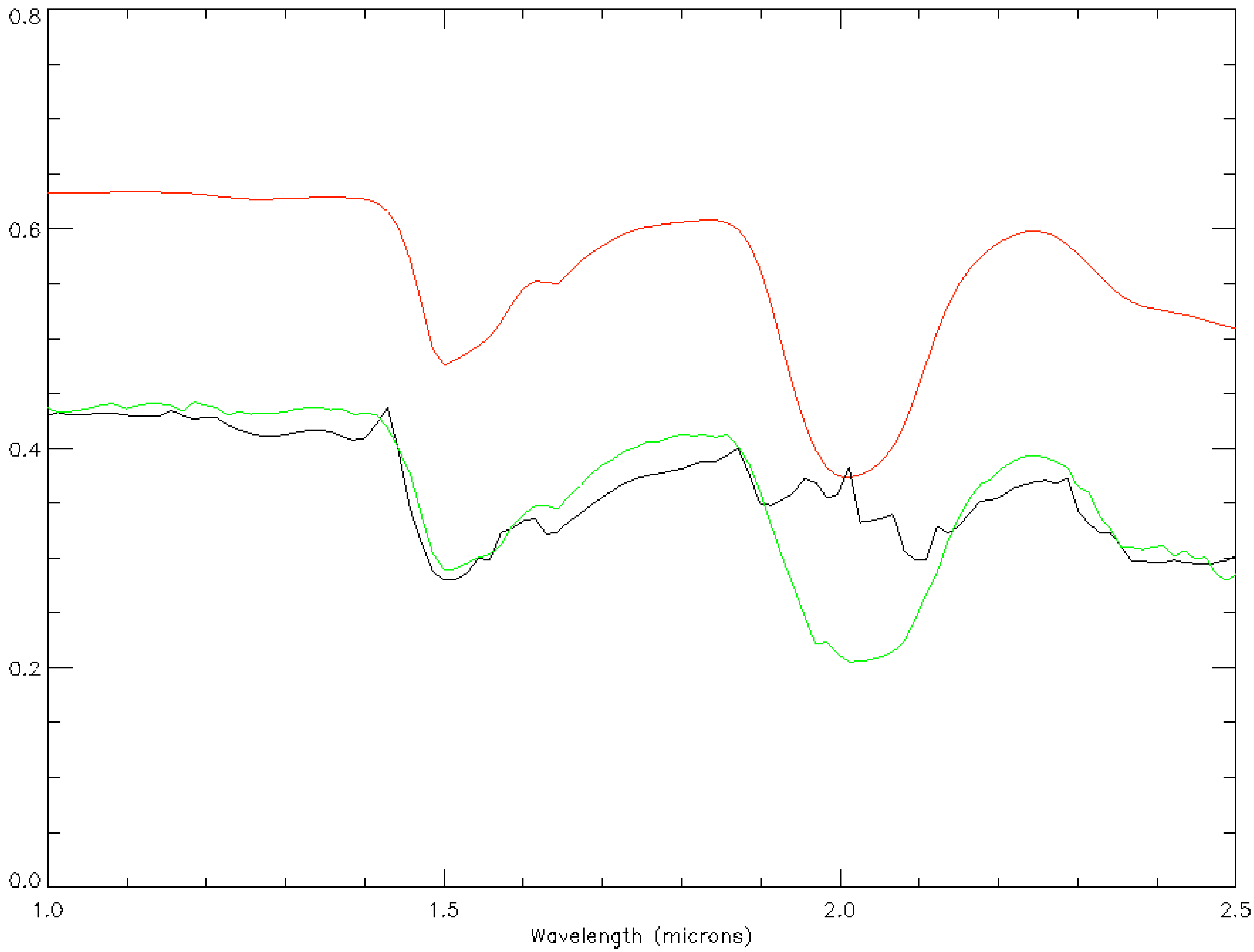

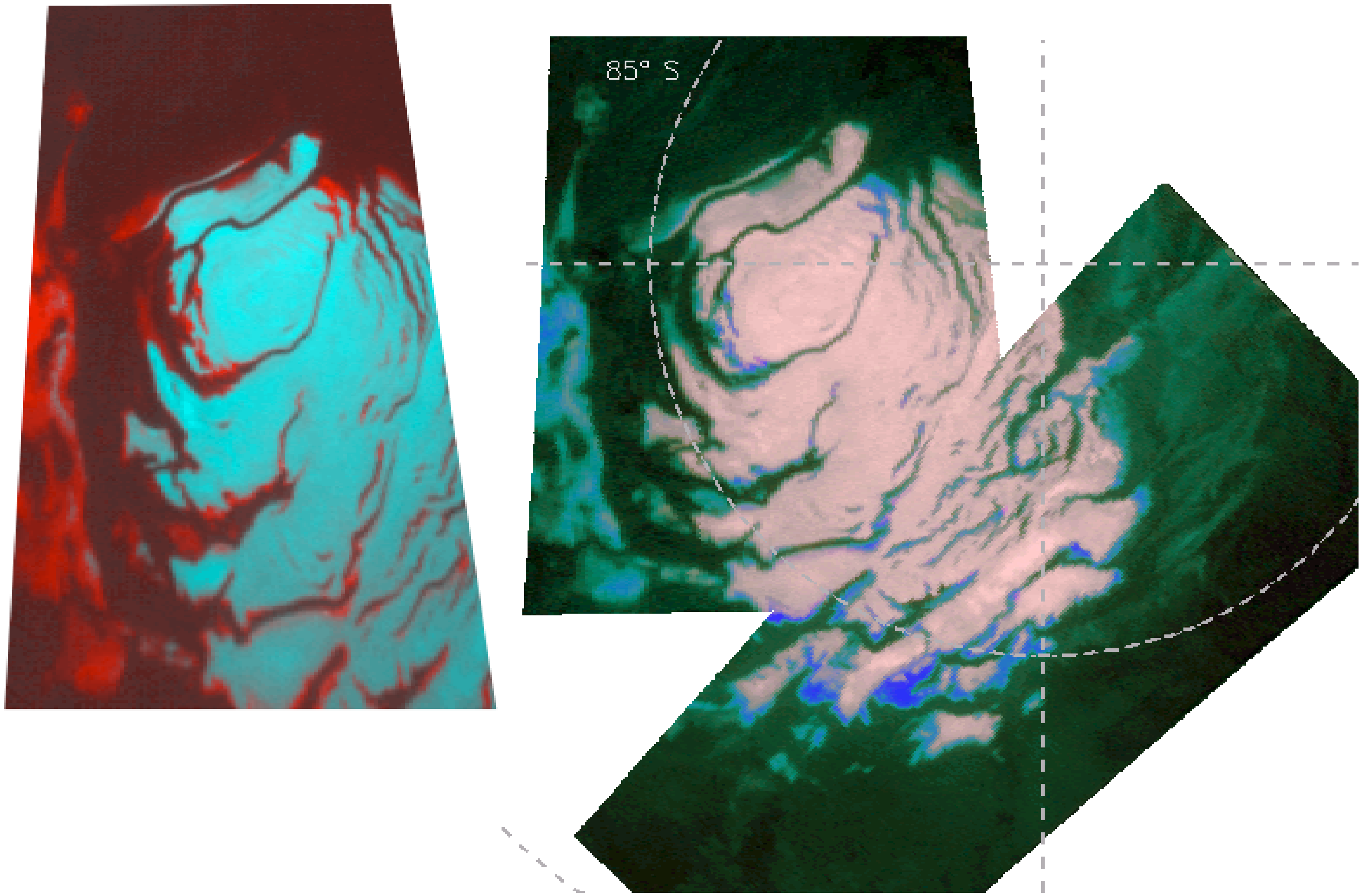
85° S

CO_2 / H_2O ICES

« SWISS CHEESE » AND/OR INTIMATE MIXTURE

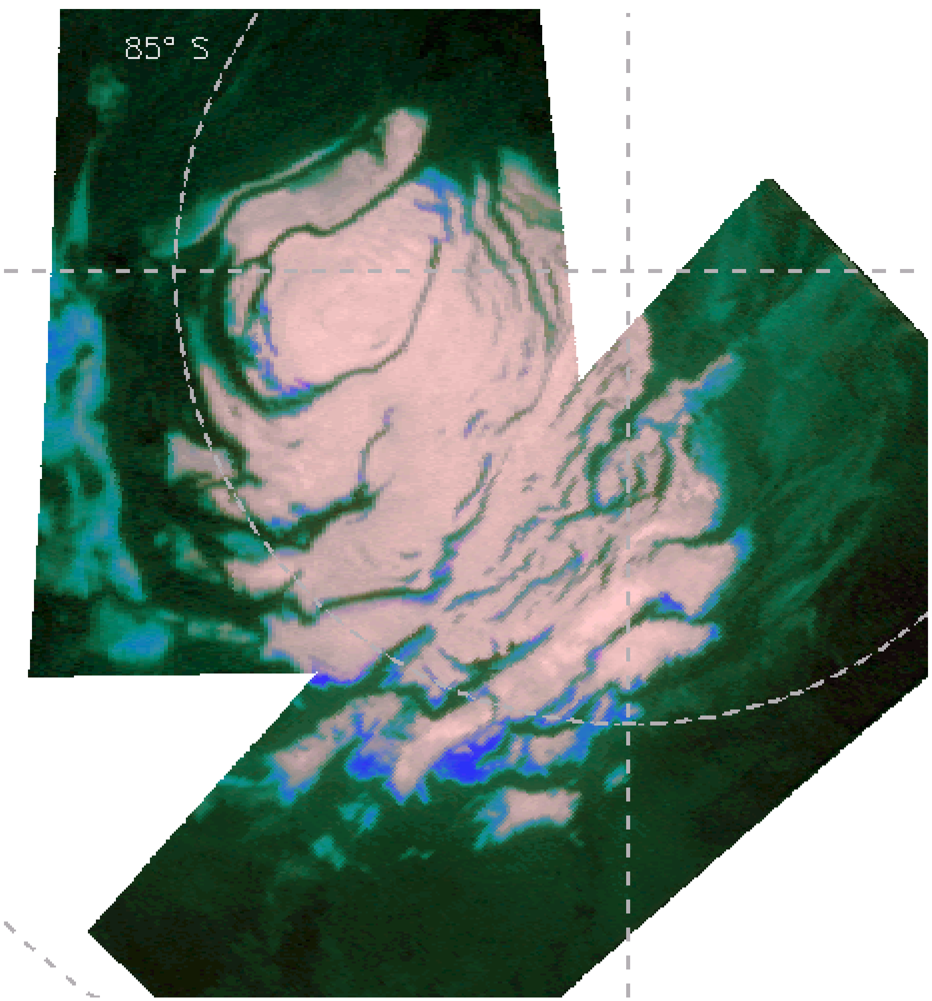

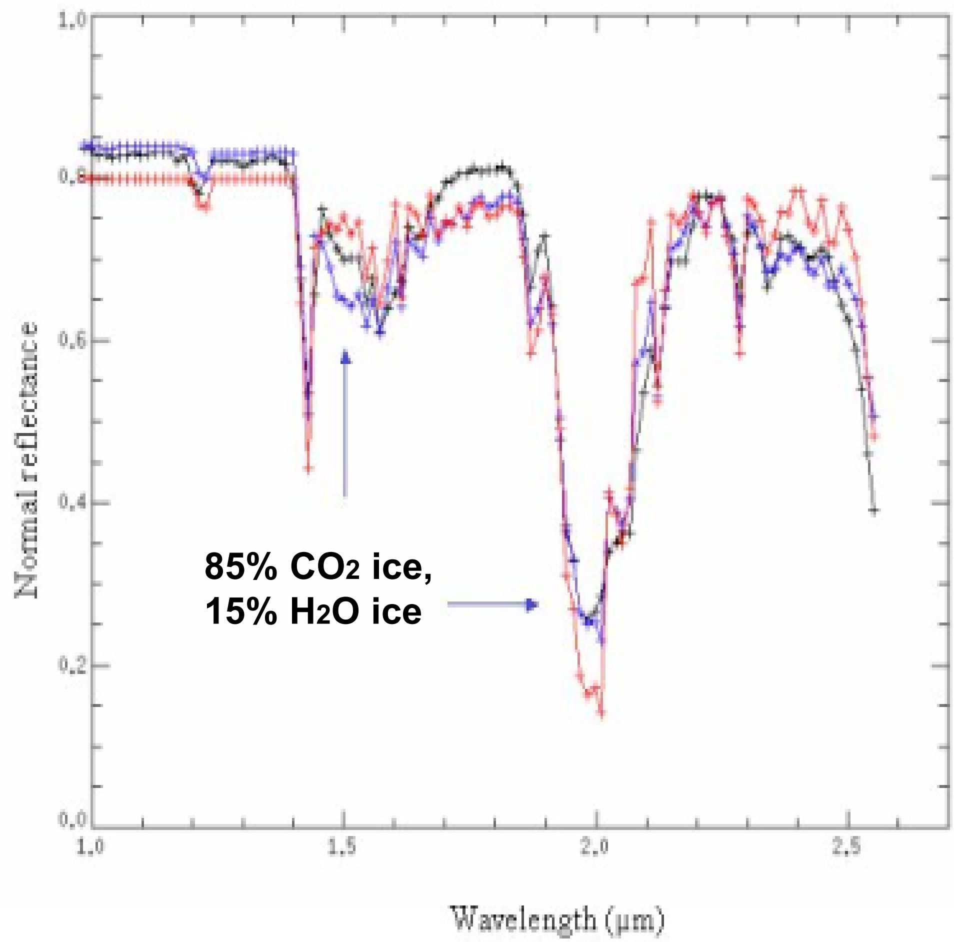

Modelling points towards an intimately mixed H_2O component in addition to the « swiss cheese » structure

Perspectives

- Discrimination of non-Gaussian signals embedded in a dominant gaussian signal.
- Identification of the sources of the non-Gaussian signal.
- Component separation.
- Use of multiscale transform as pre-processing stage for component separation techniques.